



Electron Charged Graphite-based Hydrogen Storage Material

Final Report

GTI Project number 20249

Report Issued:

March 6, 2011

Prepared For:

Mr. Jesse Adams
Project Manager
U.S., Department of Energy
Golden Field Office
Jesse.adams@go.doe.gov

Contract: DE-FG36-05GO15010

Project Period: July 1, 2005 to September 30, 2010

GTI Technical Contact:

Dr. Chinbay Q. Fan
R&D Manager
Office of Technology and Innovations
Phone: 847 768 0812
E-mail: Chinbay.fan@gastechnology.org

Gas Technology Institute
1700 S. Mount Prospect Rd.
Des Plaines, IL 60018
www.gastechnology.org

Legal Notice

This information was prepared by Gas Technology Institute (“GTI”) for the U.S. Department of Energy (“Sponsor”).

Neither GTI, the members of GTI, the Sponsor(s), nor any person acting on behalf of any of them:

a. Makes any warranty or representation, express or implied with respect to the accuracy, completeness, or usefulness of the information contained in this report, or that the use of any information, apparatus, method, or process disclosed in this report may not infringe privately-owned rights. Inasmuch as this project is experimental in nature, the technical information, results, or conclusions cannot be predicted. Conclusions and analysis of results by GTI represent GTI's opinion based on inferences from measurements and empirical relationships, which inferences and assumptions are not infallible, and with respect to which competent specialists may differ.

b. Assumes any liability with respect to the use of, or for any and all damages resulting from the use of, any information, apparatus, method, or process disclosed in this report; any other use of, or reliance on, this report by any third party is at the third party's sole risk.

c. The results within this report relate only to the items tested.

Table of Contents

Executive Summary	5
Fundamental Consideration	6
Technical Concept of Electron Charged Graphite-based Hydrogen Storage Material	6
Description of GTI / SGC Modified Material with Electron Charging	7
Storage Expectations	8
Experimental Setup	9
Results and Discussions	12
Thermo-gravimetric analysis: selection of hydrogen storage materials for electron charge experiments	12
Sievert Method	21
Technical effectiveness and Economic Feasibility	45
Actual and Goals	46
Benefit to Public	47
Summary and Recommendations	48
Figure 1. Experimental setup to measure hydrogen storage under external electron-charge	9
Figure 2. Electrode assembly	9
Figure 3. Gas phase hydrogen amount change with time under external applied voltage	11
Figure 4. Microstructure of the Expanded Graphite for Hydrogen Storage (Surface Area 700 m ² /g)	12
Figure 5. Thermo-gravimetric Analysis of the Liquid Gel Carbon Cage for Hydrogen Storage: The liquid gel carbon cage framework was doped with 10% Fe and 0.3%Pd	13
Figure 6. The effect of metal doping on the hydrogen storage capacity	14
Figure 7. The effect of catalyst on the hydrogen uptake and release rate	14
Figure 8. The improvement of the hydrogen uptake and release rate	15
Figure 9. Hydrogen Adsorption on Liquid Gel Carbon Cage Framework	15
Figure 10. Hydrogen Storage Capacities under Different Pyrolysis Temperatures	17
Figure 11. TGA Cycles of GTI High Surface Area Carbon-based Material for Hydrogen Storage without Electron-doping Material at Ambient Pressure: last quarter achievement (top) and this quarter progress (bottom)	18
Figure 12. Comparison of TGA between GTI Aero-Gel and SUNY High Surface Carbon	19
Figure 13. Modified Electron-charge Device	21
Figure 14. Hydrogen Desorption PCI Curves under Different Voltages	22
Figure 15. PCI Curve of the Carbon Cage Framework Material for Hydrogen Storage	23
Figure 16. Cyclic Voltammograms of the Hydrogen Storage Cell under Different Pressures	23
Figure 17. Electron-charge Current under Different Storage Pressures in the Hydrogen Storage Cell	24
Figure 18. PCI Curves of the Hydrogen Adsorption on Liquid Gel Carbon Cage Framework Doped with 10% Fe and 0.3%Pd, i.e. Sample A	25

Figure 19. Hydrogen Adsorption on Liquid Gel Carbon Cage Framework Doped with 10% Fe, 0.1% Pd, 10% Ti Alloy, i.e. Sample B	25
Figure 20. PCI Curves of SUNY-Syracuse Sample APKI-N3 under Different Temperatures	26
Figure 21. SEM Image of the SUNY-Syracuse Sample	26
Figure 22. SEM Element Mapping of the SUNY-Syracuse Sample	27
Figure 23. Schematic of Charged Particles for Hydrogen Storage	28
Figure 24. CCA Effect of Hydrogen Storage on the High Surface Carbon Material	28
Figure 25. External Charge Effect on the Hydrogen Storage of SUNY Sample	29
Figure 26. PCI Curve of AMTI Carbon for Hydrogen Storage at Room Temperature	30
Figure 27. PCI Curve of AMTI Carbon for Hydrogen Storage at 77K	30
Figure 28. PCI Curves of an ATMI Sample under Different Milling Times	31
Figure 29. Electro-static Voltage Effect on Hydrogen Storage at Room Temperature	32
Figure 30. Electro-static Voltage Effect on Hydrogen Storage at Room Temperature for metal modified AX-21 without a CCA	32
Figure 31. Electro-static Voltage Effect on Hydrogen Storage at 77K	33
Figure 32. Borane-Nitride Hydrogen Release at 80°C with Time	34
Figure 33. Electro-static Voltage Effect on Hydrogen Release of Borane-Nitride at 80°C and 900psi H ₂ Pressure	34
Figure 34. Cyclic Voltammogram of the Hydrogen Storage Reservoir	35
Figure 35. Electro-static Voltage Effect on Hydrogen Storage Material B-N at Room Temperature	36
Figure 36. PCI curves of the metal hydride based hydrogen storage material under different temperatures	36
Figure 37. PCI Curves at 25C under external electric charges	37
Figure 38. PCI curve with different current without cooling/heating	38
Figure 39. PCI curve with/without heating/cooling with -0.1A current	38
Figure 40. PCI curves of the electrochemical hydrogen storage device under various voltages ..	39
Figure 41. Gas phase hydrogen quantity with time under externally applied voltage	40
Figure 42. Steady state effect of external charge for hydrogen adsorption and desorption	41
Figure 43. PCI curves of hydrogen storage under different external voltages	41
Figure 44. External Charge Effect on Hydrogen Storage at Steady State	42
Figure 45. PCI curve of the metal hydride for electron-charge experiment	43
Table 1. Summary of pyrolysis temperature effect on hydrogen storage	17
Table 2. Summary of combination tested in the TGA	20
Table 3. Characterization of Charge Control Agent	28
Table 4. Summary of SUNY samples at 6300kPa	33
Table 5. Summary of External Charge Effect on JSW MH6	43
Table 6. Summary of External Charge Effect on MgH ₂	44

Executive Summary

The electron-charge effects have been demonstrated to enhance hydrogen storage capacity using materials which have inherent hydrogen storage capacities. A charge control agent (CCA) or a charge transfer agent (CTA) was applied to the hydrogen storage material to reduce internal discharge between particles in a Sievert volumetric test device. GTI has tested the device under (1) electrostatic charge mode; (2) ultra-capacitor mode; and (3) metal-hydride mode. GTI has also analyzed the charge distribution on storage materials. The charge control agent and charge transfer agent are needed to prevent internal charge leaks so that the hydrogen atoms can stay on the storage material. GTI has analyzed the hydrogen fueling tank structure, which contains an air or liquid heat exchange framework. The cooling structure is needed for hydrogen fueling/releasing. We found that the cooling structure could be used as electron-charged electrodes, which will exhibit a very uniform charge distribution (because the cooling system needs to remove heat uniformly). Therefore, the electron-charge concept does not have any burden of cost and weight for the hydrogen storage tank system.

The energy consumption for the electron-charge enhancement method is quite low or omitted for electrostatic mode and ultra-capacitor mode in comparison of other hydrogen storage methods; however, it could be high for the battery mode.

Fundamental Consideration

Technical Concept of Electron Charged Graphite-based Hydrogen Storage Material

The Gas Technology Institute (GTI) and Superior Graphite Company (SGC) developed a concept for materials to store hydrogen for transportation vehicles and other applications based on low cost natural flake graphite materials with modifications. An effective hydrogen storage system for transportation applications requires quick charge and discharge, high wt% storage capacity with small volumes, durability over many cycles, and safe handling and transport.

This concept involves modification of low cost natural flake graphite for hydrogen storage using the following three key steps.

1. Expansion of the graphite layers to allow access for hydrogen adsorption.
2. Metal intercalation in the graphite layers to increase back-donated electron charges onto the carbon, so that the hydrogen adsorption becomes combined physisorption and chemisorption.
3. Addition of electron charge in the process of hydrogen filling (using a process similar to copying machine systems).

The GTI hydrogen storage concept is a combination of physisorption and chemisorption with the use of an externally applied electron charge during filling. The presence of the metal doping augments hydrogen uptake by hydriding, however its presence is designed to donate electrons and maintain the expanded graphite structure. Without the intercalated metal, the required electron charges needed for this approach would be very high. This hydrogen storage concept is expected to function at normal fueling temperatures.

The Gas Technology Institute and Superior Graphite Company base this concept for new materials to store hydrogen on-board vehicles and other applications on low cost graphite materials that are modified through specifically tailored processing steps.

An effective hydrogen storage system for transportation applications requires quick fueling and release, high weight% storage capacity using small volumes, high durability over many cycles, and safe handling and transport.

Hydrogen storage on carbon-based adsorbents has been investigated since the 1960's. These carbon-based materials included graphite, nanocarbon fibers (NCF), fullerenes, carbon nanotubes (CNT), and nanohorns. A report from NREL (in Proceedings of the 2001 DOE Hydrogen Program Review) summarized the progress and experimental details on carbon nanotube materials for hydrogen storage. This report concluded that typical hydrogen storage capacities on the carbon single-wall nanotubes range from 2-4-wt%. Metal hydrides are in the same range, generally under 3 wt%.

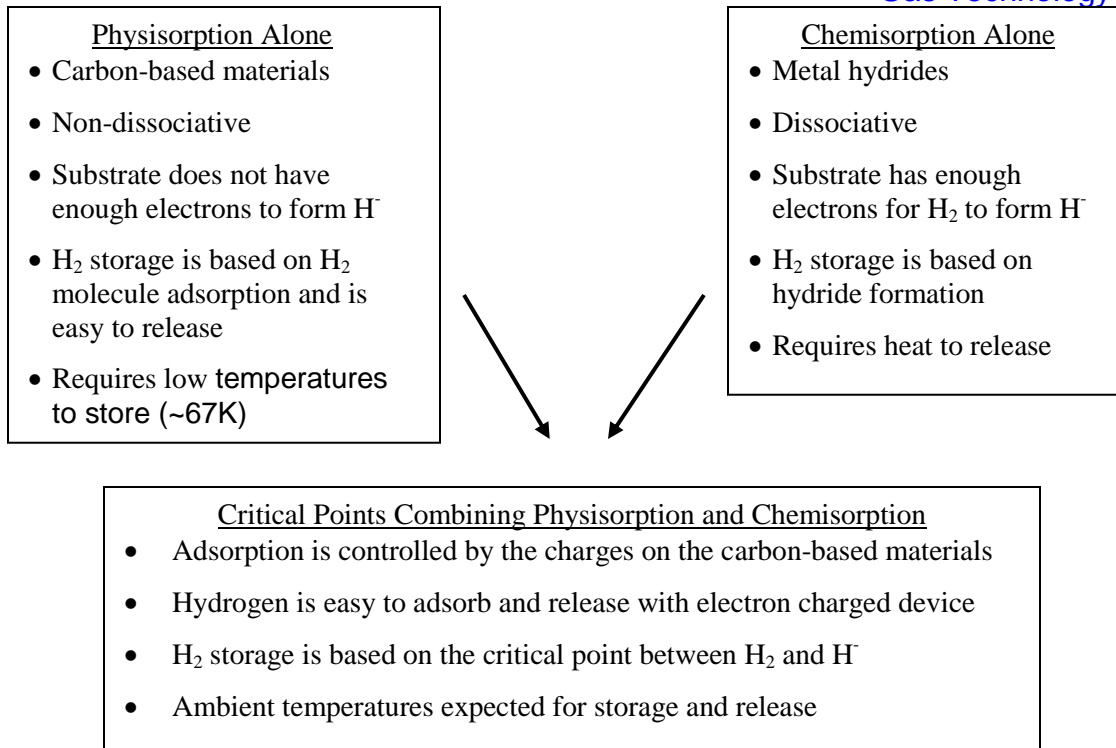
In a different direction, leading to a better understanding of our concept, a theoretical study by Pederson and Broughton (in Science News, 14, 327, 1992) found that the adsorption forces for polarizable molecules, such as HF, on fullerene tubes would be stronger than on ordinary graphite. They also found that the carbon nanotubes had highly "polarizable molecular straws", which enables an ingestion of dipolar molecules. It is not hard to imagine that the polarized carbon based materials would have a stronger adsorption force for "polarizable" molecules.

In the last ten years, the main focus was on the investigation of such tubular shape molecules for hydrogen storage, which showed some promising results. The modifications of these molecules were also most interesting. However, the cost of these materials is very high, and the hydrogen storage within these materials seemed not yet to be easily reproducible. Furthermore, the temperature for hydrogen storage using these materials needs to be quite low. Johnson et al. (in *Journal of Chemical Physics*, 111, 9778, 1999) concluded, “Even charged nanotube arrays are not suitable sorbents for achieving the DOE target for hydrogen transportation and storage at near ambient temperatures, unless the charges on the nanotubes are unrealistically large”. Although the experimental results to date have been different from theoretical studies, we believe that graphite carbon-based materials are still the best option to pursue due to their mechanical strength, reliable, availability, and potentially very low cost.

Description of GTI / SGC Modified Material with Electron Charging

Hydrogen is a non-polar molecule and it is physisorbed on carbon-based materials. The carbon materials are also non-polar substrates. The non-polar hydrogen molecules adsorbed on non-polar carbon substrates are not dissociated and the force binding these two non-polar species is essentially weak van der Waals forces. However, as previous research has shown, the adsorption force could increase if the substrate could be polarized. The polarization of the substrate can be done in two ways. One way is to deposit, or intercalate electron-rich materials such as metals, or “electron-hungry” materials, such as nitrogen, phosphorus and other atoms. These methods are possible with the graphite layer expanding techniques developed by Superior Graphite. Another way is to polarize the entire substrate by adding an electrical potential similar to capacitors. In this concept, either intercalation or charging alone is not sufficient to achieve high storage capacities. Therefore, we propose to combine a method of polarization with the modified expanded intercalated graphite structure. We believe this to have an excellent chance to meet the DOE hydrogen storage targets at ambient temperatures.

To insure that sufficient charge electrons are available, an electrical potential is applied to this structure when adsorbing the hydrogen onto the material. Dissipating the charge aids the release of the stored hydrogen. Restating as Johnson et al. pointed out, the carbon-based material needs a sufficient charge ($0.1e^-/C$) for meaningful hydrogen adsorption at room temperature. Metal intercalation as an electron donor source alone might not supply sufficient charge. As a result we propose to add charges on the restructured graphite materials during filling, using a process similar to copying machines where an electron charge device temporarily charges the copier’s carbon particles. By applying a charge to the graphite-based hydrogen storage material, we will be able to back-donate more charges on the carbon so that hydrogen molecules can be sufficiently adsorbed. The charge could be dissipated immediately after the container is filled. The added charge will increase the hydrogen adsorption on the modified graphite, but the question of whether it is enough has to be determined experimentally along with optimization of structures.



GTI and SGC Combination Concept for Hydrogen Storage

An electron charged cage similar to a Faraday cage consists of an inner wire mesh cylinder as a device charge distributor and container, and an outer cylinder. When charged graphite materials are inside the closed conducting mesh cylinder, they produce equal charges on the outside of the cylinder surface. When the charge is applied, it brings charges to the inner surface, which immediately balances to the inside graphite-based materials, having the same amount of charges. A potential is produced between the inner mesh cylinder and the outside tank cylinder. To prevent discharge between the inner and outer cylinder, an insulation layer will be placed between the two layers. When the inner cylinder is charged, the carbon-based materials are charged; then hydrogen is filled into the cylinder.

Storage Expectations

The graphite material structure becomes basically expanded and in twisted layers. Hydrogen can be adsorbed on both sides of the many layers, thus one carbon atom could possibly adsorb two hydrogen molecules when the hydrogen molecules are perpendicular to the carbon layer (using the terms of surface chemistry). Theoretically, assuming a monolayer adsorption, when the hydrogen molecules are parallel to the carbon layer the maximum hydrogen storage is 14 wt%. However, metal doping into the graphite layers will increase the weight and all sites may not hold hydrogen, thus the hydrogen storage will be less than 14 wt%. Optimization of the amount of metal doping, the acid treatment steps, and quantity of charge are essential to maximizing the hydrogen storage capacity of the system.

Experimental Setup

The main experimental setup is the Sievert device with a hydrogen storage reservoir, which is connected to the external charge instrument. Figure 1 shows the diagrams of the setup. Generally the device is composed of electrode assembly as shown in figure 2. The anode side is composed of AB₅ type metal hydride pressed onto perforated nickel sheet with a binder. The cathode side is composed of a nickel pin with Ni oxide composites. The separator is a porous polymer, which is either dry (electrostatic mode) or soaked with KOH solution (ultracapacitor mode and battery mode). The layered electrode assembly was rolled up to a cylindrical shape and a layer of insulator was added to prevent shorting between the anode and the cathode.

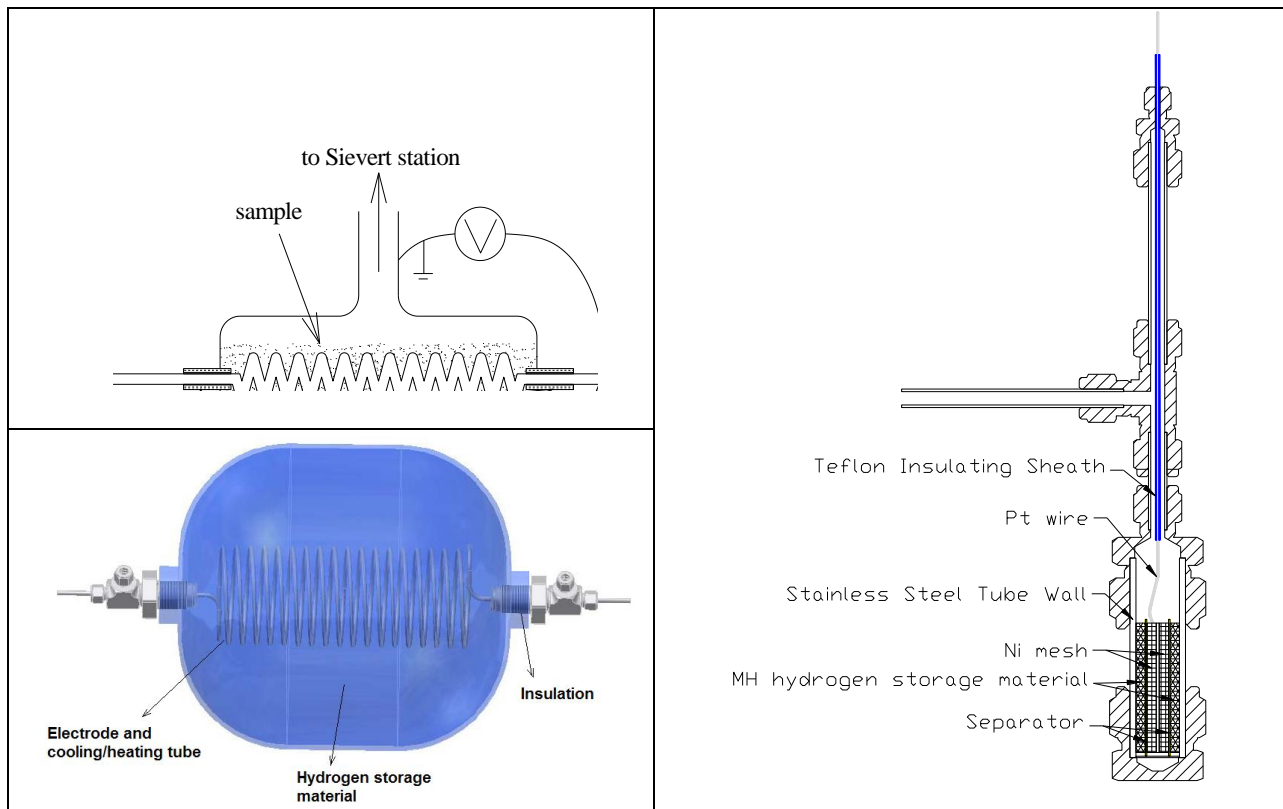


Figure 1. Experimental setup to measure hydrogen storage under external electron-charge

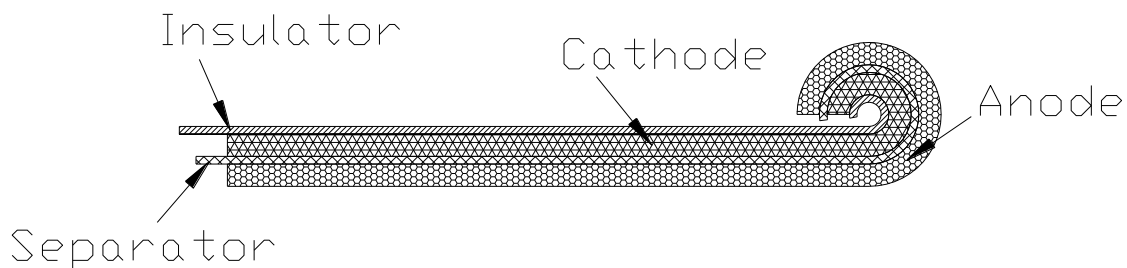


Figure 2. Electrode assembly

The following is a standard test procedure of the Sievert method.

- Step 1: Use He calibrate sample vessel dead volume; Keep sample vessel in ice water; Vacuum system.
- Step 2: Apply H₂ to system and obtain equilibrium pressure 138psig without external charge.

Constant Voltage cycle:

- Step 3: Apply 1.5V to the pin electrode vs. sample vessel wall. Record system pressure change as function of time. System pressure goes up as high as 157.7 psig.
- Step 4: Apply 0.8V to pin electrode vs. sample vessel wall. Record system pressure change as function of time. System pressure goes down to 116.6psig.

Constant current cycle:

- Step 5: Apply constant current of -200mA for 2 hours. Record system pressure change as function of time. System pressure goes up to 141.1psig.
- Step 6: Apply constant current of +200mA. Record system pressure change as function of time until voltage drops very quickly below 0.7V. The total time of applied 200mA is about 2 hours. System pressure goes down to 121.8 psig. Calculate gas phase mole number at time of each experiment condition

The rolled electrode assembly was put into the electro-charge sample vessel as shown in figure 2. There was a Pt wire connected to the cathode of the electrode assembly. The anode of the electrode assembly was in contact with the sample vessel which was made from stainless steel. Between the anode and sample vessel, there was extra metal hydride material filling the void. The sample vessel was connected to a Sievert apparatus for the hydrogen storage test. The cathode was connected to a working electrode; the anode/sample vessel wall was connected to a reference electrode and counter electrode. High pressure hydrogen (above 600psig) was applied to the system and then released to ambient pressure three times for activation.

The sample vessel was kept in a 0°C temperature bath and the hydrogen storage testing was carried out first by applying voltage or current to the vessel. The initial pressure of the system was equilibrated at around 150psig. A voltage higher than Open Current Voltage (OCV) was first applied to the cathode vs. the anode and the pressure change was recorded. Then a voltage lower than OCV was applied to the cathode vs. the anode and the pressure change was recorded. The result is shown in figure 3. After electro-charge the system pressure was brought down to around 10 psig and a pressure-composition isotherm (PCI) curve was acquired at OCV. When comparing the electro-charge and PCI results it is clear that the electro-charge can result in a larger hydrogen mole number change than PCI shown at OCV, even if more hydrogen pressure was applied at OCV. This is a sign that electro-charge can affect hydrogen storage in this system.

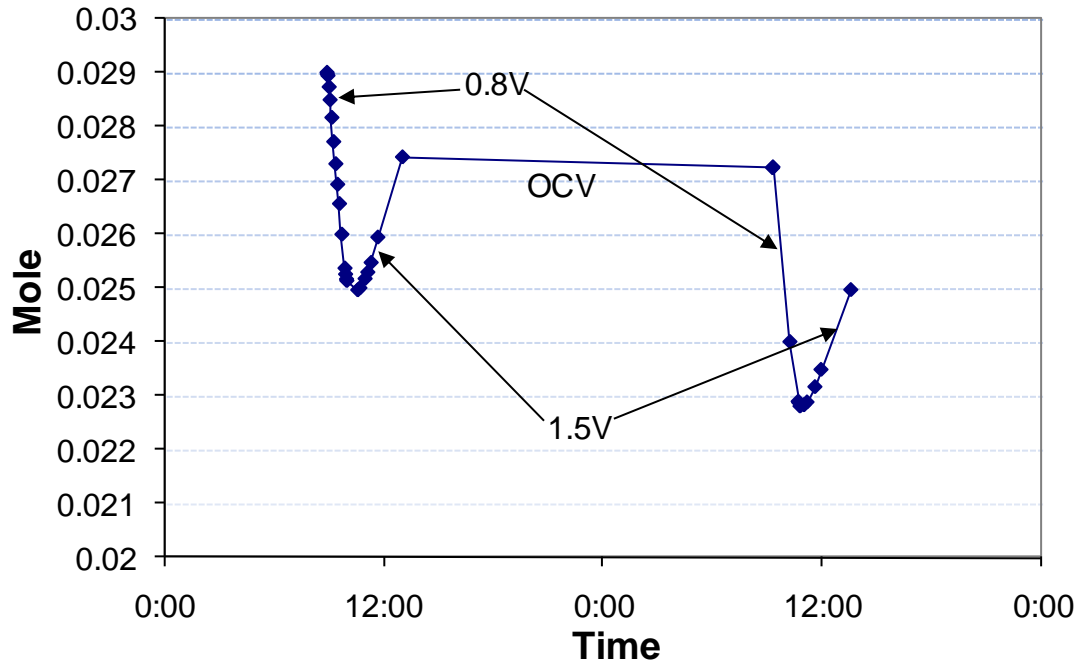


Figure 3. Gas phase hydrogen amount change with time under external applied voltage.

The hydrogen storage materials selected for the electron charge tests were first examined using dynamic thermo-gravimetric analysis (TGA). The dynamic TGA TherMax 500 was made by Thermo Cahn and allows for high pressure (up to 1000 psi) and high temperature (up to 1000°C). A series of materials, such as high surface carbon from State University of New York (SUNY) at Syracuse, metal hydrides from Japan Steel Work (JSW), and Advanced Technology Materials, Inc. (ATMI) were evaluated. The TGA screen results were compared with Sievert method tests to justify the electron-charge effects on the hydrogen storage capacities.

Results and Discussions

Thermo-gravimetric analysis: selection of hydrogen storage materials for electron charge experiments

(1). Exfoliated graphite

GTI worked with its partners, Superior Graphite and specific equipment at the University of Massachusetts to develop the graphite based hydrogen storage materials. Figure 4 shows the images of the expanded graphite based materials and TGA of the hydrogen uptake. We have achieved 4.5Å spacing between graphite flakes for hydrogen uptake.

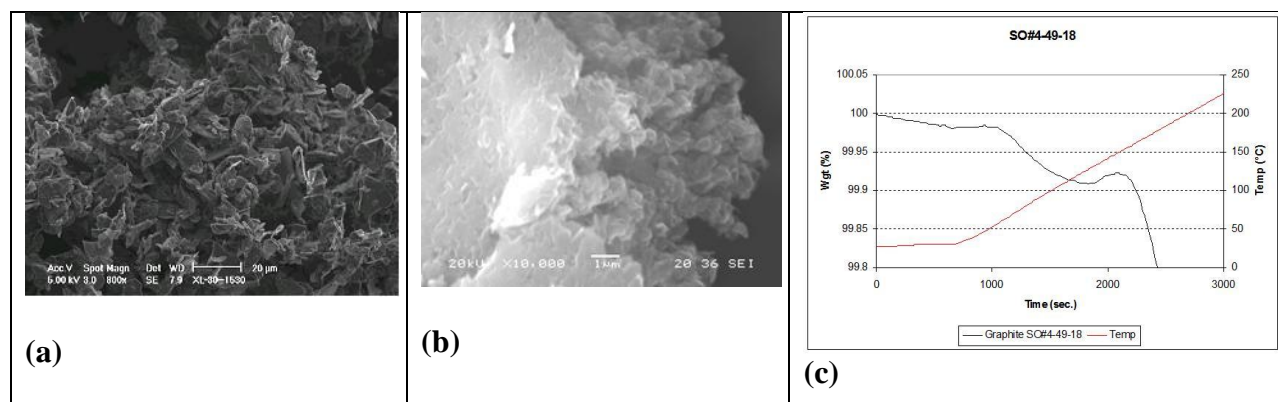


Figure 4. Microstructure of the Expanded Graphite for Hydrogen Storage (Surface Area 700 m²/g)

Figure 4 (a) and (b) are images of a unique graphite which possess a very high surface area unlike previous graphite materials. Figure 4 (c) shows the preliminary data of the expanded graphite hydrogen storage. An interesting peak was observed at 120°C. This peak could be a hydrogen uptake peak.

(2) Liquid gel carbon

Liquid gel carbon was prepared chemically. Potassium carbonate (1.29g) was added to a suspension of 2,4-dihydroxybenzoic acid (2.9g, Sigma-Aldrich) in deionized water (100ml). The suspension was stirred until the reaction was fully complete upon which the solution was completely clear. Then formaldehyde (3g, 37% solution in water) or glutaric acid (GA) was added to the solution and K₂CO₃ (26mg) was added as a catalyst. The solution was put into a capped glass bottle and set for 24 hours at room temperature followed by 72 hours at 80°C. A potassium ion loaded dark red hydrogel was formed after the above steps. This dark red hydrogel was then ion exchanged with 0.1M metal salt solution three times, each time for 24 hours. The metal salt solution in our case is 0.1 M Fe(NO₃)₃ or Fe(NO₃)₂. After the ion exchange process, the hydrogel was then washed with DI water, acetone and soaked in acetone to exchange water in the hydrogel with acetone.

The resulting gel was subjected to 900°C for 3 hours under an inert gas atmosphere for pyrolysis and then treated with hydrogen at 330°C for 1 hour for activation. The sample was then put into the TGA under a hydrogen atmosphere for testing.

The TGA data of the liquid gel carbon for hydrogen storage is displayed in Figure 5. The results demonstrate that the hydrogen storage material has a memory effect, which causes the hydrogen storage capacity to decrease with cycling. More tests are needed to establish the degree of the loss of storage capacity with cycles. Figure 6 shows the improvement of the hydrogen storage capacity when metals are added to the carbon material and Figure 7 shows the improvement of the hydrogen adsorption and desorption rate. The hydrogen storage capacity increased after modification of the carbon-based material with different metal doping. We added 5% Pd catalyst to the material and found the hydrogen desorption rate increases rapidly.

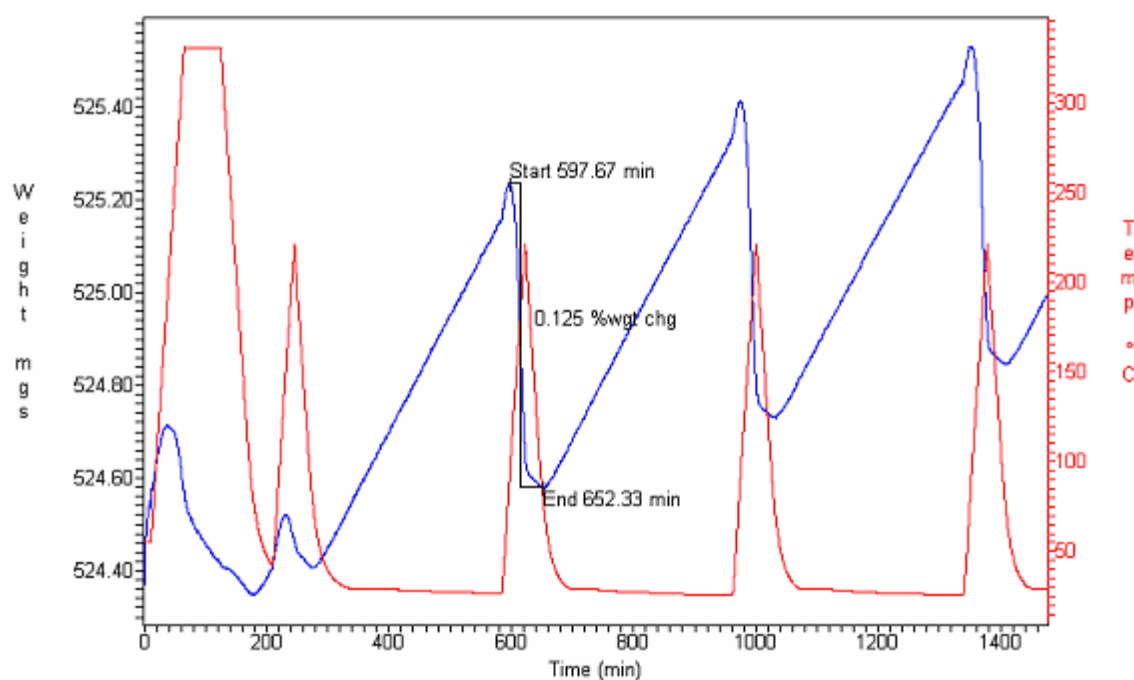


Figure 5. Thermo-gravimetric Analysis of the Liquid Gel Carbon Cage for Hydrogen Storage: The liquid gel carbon cage framework was doped with 10% Fe and 0.3%Pd

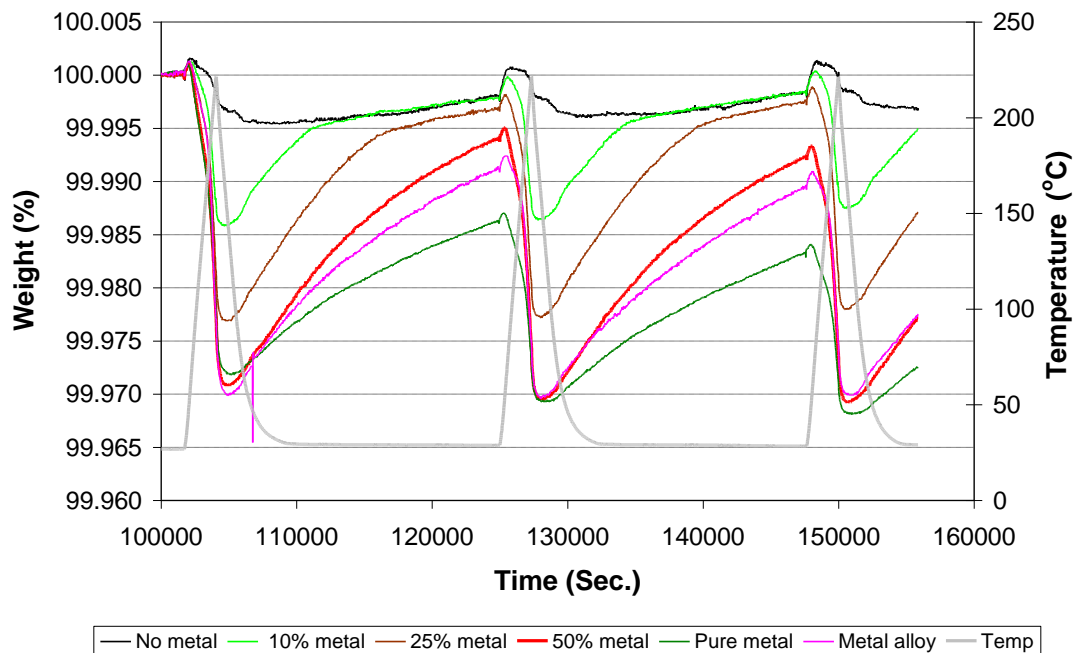


Figure 6. The effect of metal doping on the hydrogen storage capacity

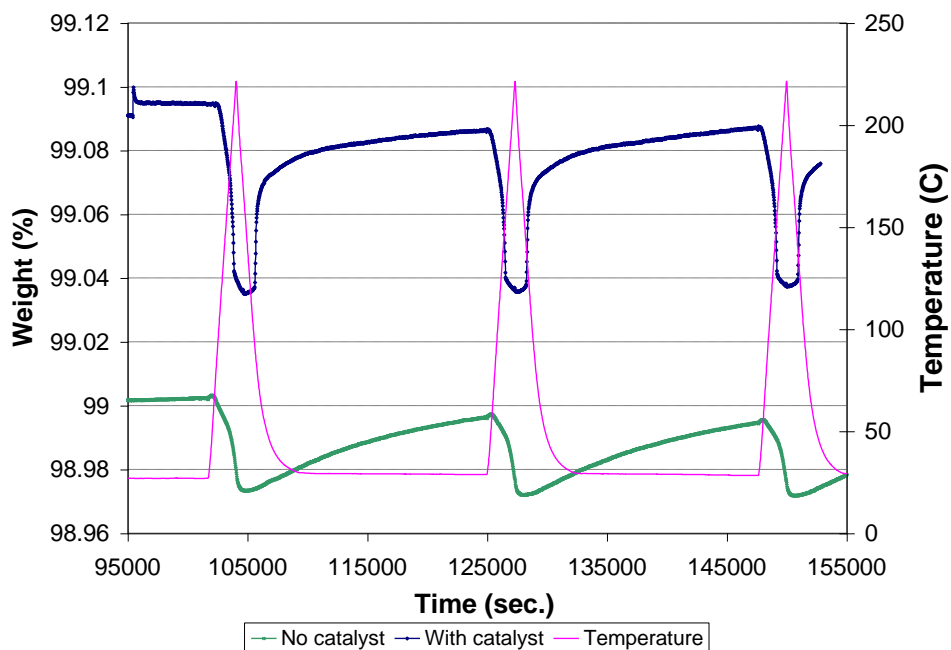


Figure 7. The effect of catalyst on the hydrogen uptake and release rate

Figure 8 and 9 show the improvement of the hydrogen adsorption and desorption rate with different doping amount of metal. The hydrogen storage capacity increased after modification of the carbon-based material with different metal doping. The sample showed a reversible weight gain and loss of about 0.13wt% during the 220°C heat cycle. This increase is not significant,

especially at high pressure. Thus we prepared a series of modifications. Meanwhile, we synthesized high surface carbon aerogels and liquid gels. Dynamic TGA was used to screen the hydrogen storage capacity at ambient pressure. Figure 10 shows the hydrogen storage charge/discharge cycles. Since the Dynamic TGA is very precise and no water condensation affects the test, we were able to quickly obtain the storage capacity changes due to different modifications. Table 1 summarizes the results of the TGA. The pyrolysis temperature affects the hydrogen storage capacity at ambient pressure.

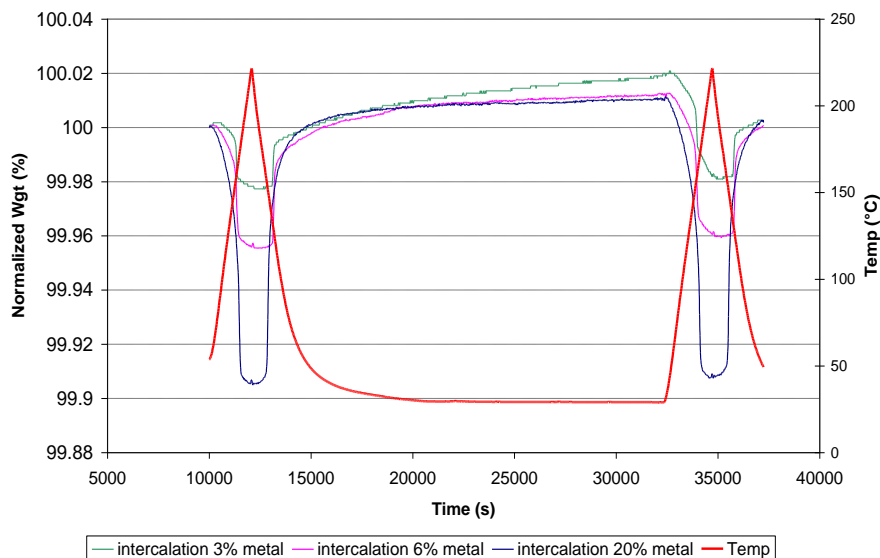


Figure 8. The improvement of the hydrogen uptake and release rate

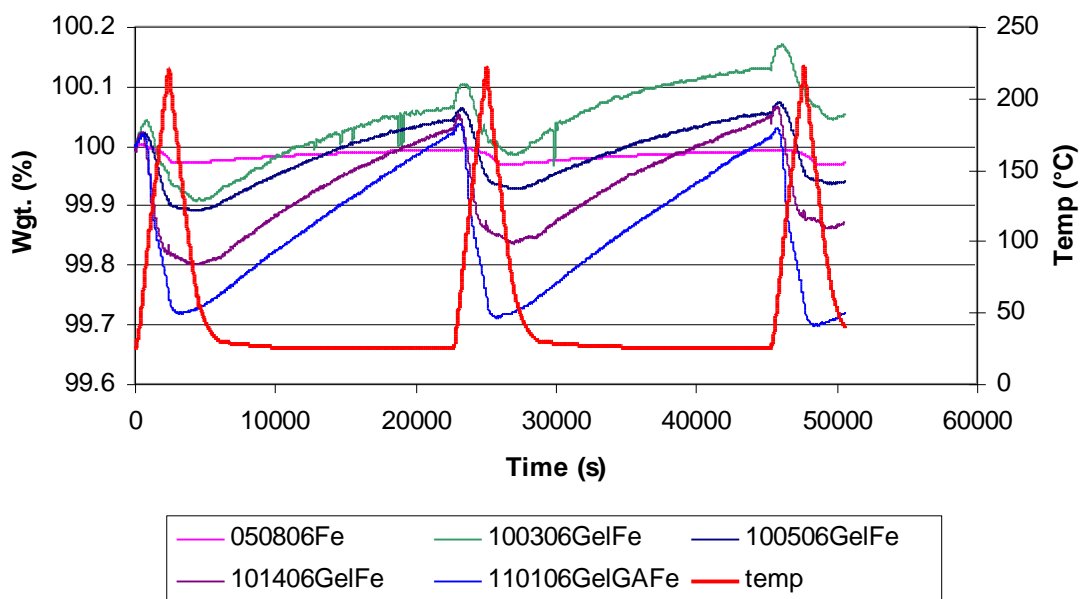
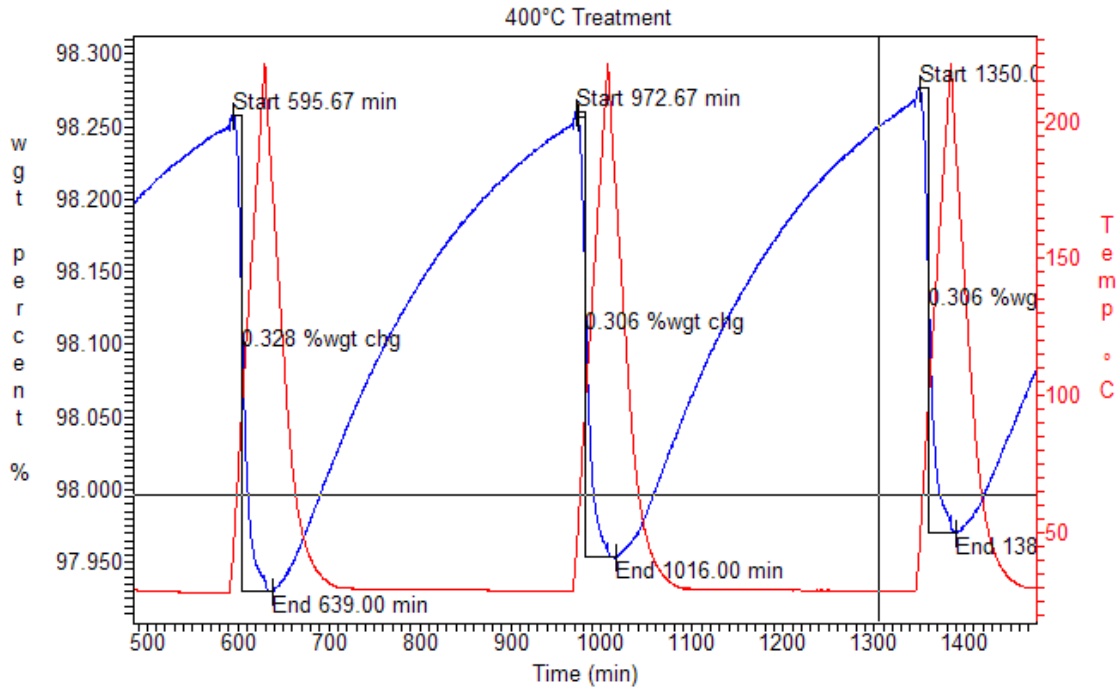
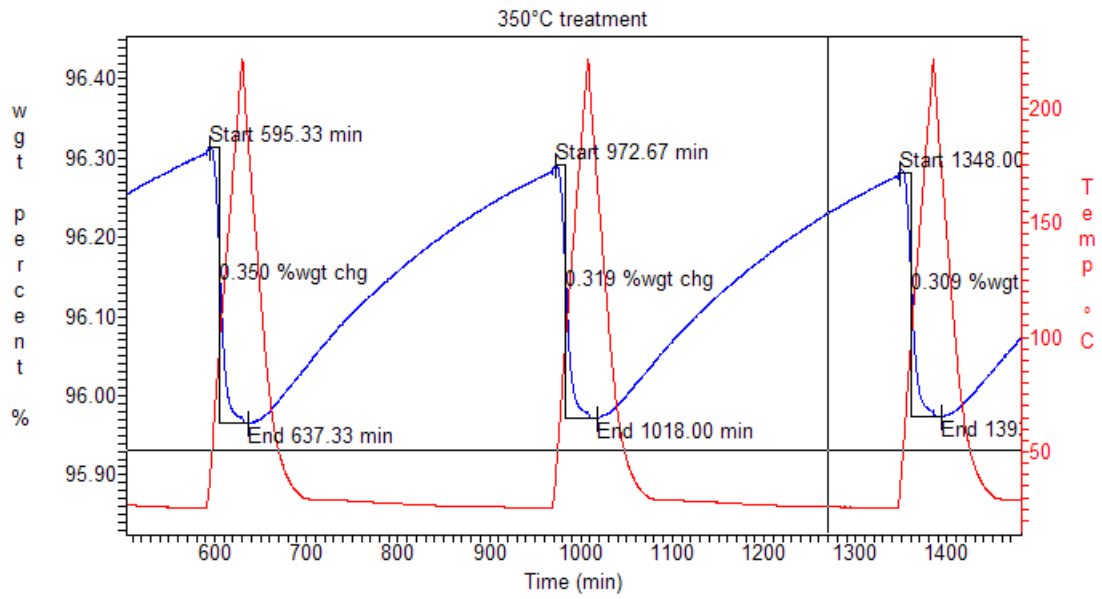


Figure 9. Hydrogen Adsorption on Liquid Gel Carbon Cage Framework



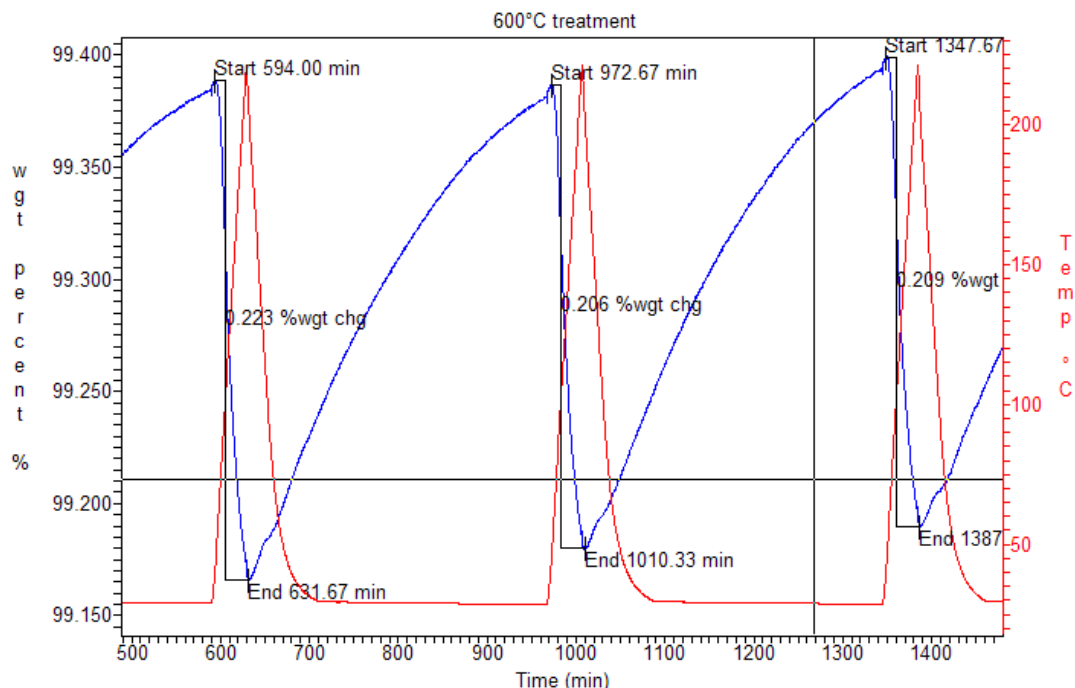


Figure 10. Hydrogen Storage Capacities under Different Pyrolysis Temperatures

Table 1. Summary of pyrolysis temperature effect on hydrogen storage

Pyrolysis Temperature (°C)	Hydrogen Storage (wt%) (1 st Cycle)	Hydrogen storage (wt%) (2 nd cycle)
350	0.350	0.319
400	0.328	0.306
600	0.223	0.206

The carbon-based materials were modified with Fe and Pd electron-rich materials. This doping resulted in doubled the hydrogen storage capacity to 1.325 wt.% with Fe/Pd treatment from 0.796 wt.% with only Fe treatment. These results showed much better performance than untreated as shown in Table 1. Figure 11 shows TGA cycles of GTI high surface area carbon-based material for hydrogen storage at ambient pressure.

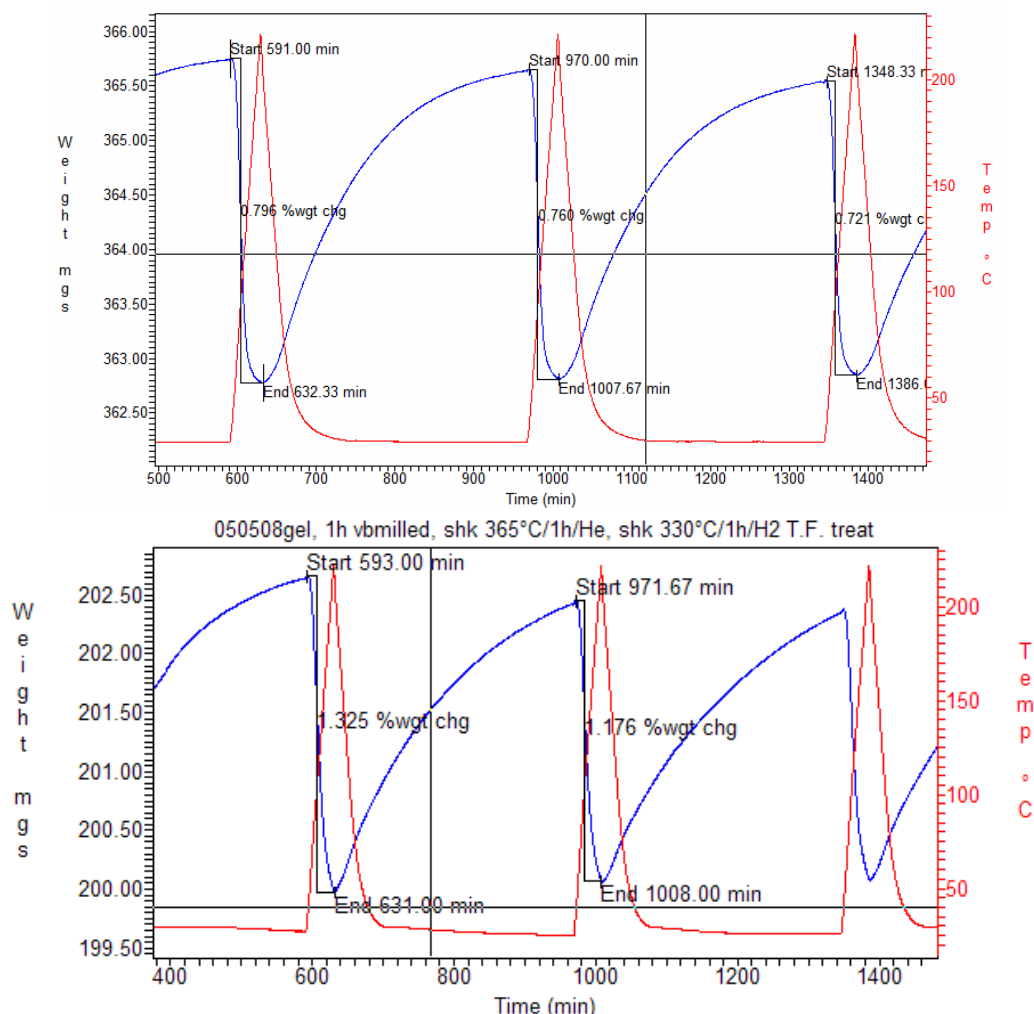


Figure 11. TGA Cycles of GTI High Surface Area Carbon-based Material for Hydrogen Storage without Electron-doping Material at Ambient Pressure: with only Fe treatment (top) and with Fe/Pd treatment (bottom)

(3) High surface carbon from customers (SUNY at Syracuse and AX-21)

In order to improve the electron charge effect on the hydrogen storage, we charged the material particle surface as shown in Figure 12. Prof. Cabasso of SUNY at Syracuse offered us samples to test in both TGA and Sievert devices. For comparison, GTI's aero-gel carbon was tested under the same conditions as the high surface carbon from SUNY.

The SUNY sample of PKMK Bulk, which showed 0.59wt% at 60bar at room temperature, was also tested in TGA. The TGA temperature profile was heating to 330°C and kept for 1h then cool down followed by 220°C heating cycles. During the test, hydrogen was the reaction gas inside TGA furnace without any back pressure. The result is shown below in Figure 12. The aerogel showed 1.3wt% reversible weight loss/gain. The PKMP bulk (SUNY sample) showed 0.056wt% weight loss/gain.

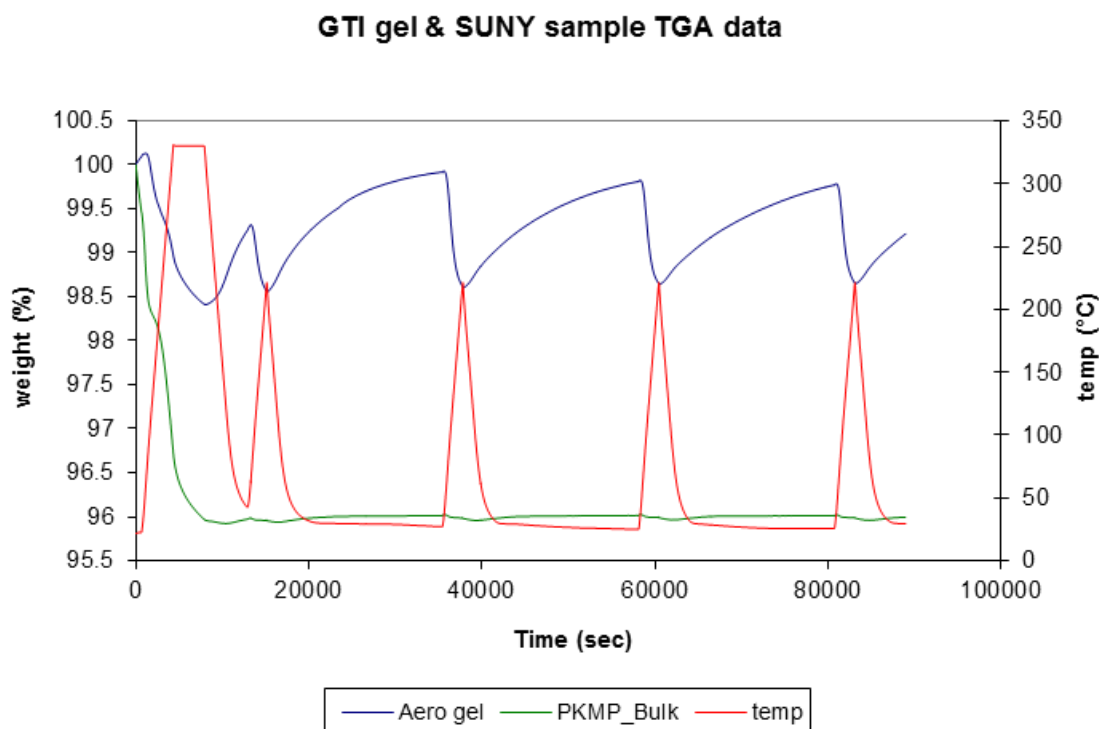


Figure 12. Comparison of TGA between GTI Aero-Gel and SUNY High Surface Carbon

(4) Borane nitride

We screened borane-ammonia based samples for hydrogen storage in both TGA and Sievert station. Very interesting data were obtained and listed in Table 2. Theoretically, ammonia borane contains 20% hydrogen and fully decomposes at high temperatures. With different doping, the hydrogen release rate increases tremendously. We are striving to make the electric charge to get the reverse reaction to occur; i.e. H₂ adsorption. A summary of the combinations that we have tested in the TGA is provided in table 2. The weight loss was assumed as the hydrogen release, however, the residue analysis needs to be performed.

Table 2. Summary of combination tested in the TGA

Sample content	Weight loss after 150°C (%)
BH ₃ NH ₃ :MH (1:2)	6.895
BH ₃ NH ₃ :MH (1:2) after 650psig activation at RT	5.06
BH ₃ NH ₃ :CoPYY (1:2)	4.6 (130°C)
BH ₃ NH ₃ :Ni (1:1)	13.828
BH ₃ NH ₃ :SAPO (1:1)	15.292
BH ₃ NH ₃ :BiPbSnCd (1:1)	10.26
BH ₃ NH ₃ :BZSM5 (1:1)	10.663
BH ₃ NH ₃ :BZSM5 with Rh (1:1)	9.742
BH ₃ NH ₃ :KA (1:1)	13.555
BH ₃ NH ₃ :BiSn (1:1)	9.008
BH ₃ NH ₃ :Silicalite (1:1)	13.555
BH ₃ NH ₃ :LaNi ₅ (1:1)	8.583
BH ₃ NH ₃ :Al:SAPO (2:1:1)	13.599
BH ₃ NH ₃ :Fe:SAPO (2:1:1)	14.449
BH ₃ NH ₃ :TiH ₂ :SAPO (2:1:1)	12.622
BH ₃ NH ₃ :NiFe:SAPO (2:1:1)	12.167
BH ₃ NH ₃ :PdCl ₂ :SAPO (2:1:1) ^{mixture reacted}	12.167
BH ₃ NH ₃ :FeTiO ₃ :SAPO (2:1:1)	10.92
BH ₃ NH ₃ :Fe _x N:SAPO (2:1:1) _{x=2~4}	12.362
BH ₃ NH ₃ :SiC:Rh (15:11:4)	8.662
BH ₃ NH ₃ :hydroquinone:Rh (15:10:5)	7.773
BH ₃ NH ₃ :Polyaniline emeraldine (1:1)	10.556
BH ₃ NH ₃ :BZSM5:Ag/C (15:10:5)	11.273
BH ₃ NH ₃ :TiC:BZSM5 (2:1:1)	8.826
BH ₃ NH ₃ :Pyrene:Rh (15:15:1)	8.4
BH ₃ NH ₃ :Pyrene:Ni (15:15:1)	7.741
BH ₃ NH ₃ :Pyrene:PdCl(PPh ₃) ₂ (15:15:2)	8.266
BH ₃ NH ₃ :CoPYY/C:RhCl(PPh ₃) ₃ (15:15:2)	12.546
BH ₃ NH ₃ :CoPYY/C:V:RhCl(PPh ₃) ₃ (15:8:7:2)	12.059%
BH ₃ NH ₃ :LiAlH ₄ (3:1)	14.034%
BH ₃ NH ₃ :NaBH ₄ (3:1)	14.153%
BH ₃ NH ₃ :LiAlH ₄ (1:1)	19.677% (100°C)
BH ₃ NH ₃ :LiAlH ₄ :MH (3:1:2)	13.341%
BH ₃ NH ₃ :LiAlH ₄ :Graphene (3:1:2)	10.04%

Sievert Method

After the section of materials for hydrogen storage by TGA, the Sievert method is used to evaluate hydrogen storage pressure-composition-isotherm (PCI) curves. An electric charge sample vessel capable of acquiring a PCI curve under liquid nitrogen temperature was designed and made as shown in Figure 13.



Figure 13. Modified Electron-charge Device

1) System verification

Initially, a metal intercalated graphite material was tested and obtained from 0.8 to 1 wt.% hydrogen storage to calibrate the Sievert instrument. Figure 14 contains the PCI curves for this experiment. The applied electron-charge mainly affects the physical adsorption regions. We have repeatedly found that the application of a negative charge shifts the PCT to right (increases hydrogen adsorption) while the application of a positive charge shifts the PCI curve to left (decrease hydrogen storage). In these tests the device temperature was fixed at room temperature and the tests were repeated six times. However, the electron-charge effect on AB2 and AB5 storage materials is limited. We believe the PCI shift is related to the electronic structure of the substrate. Electron-rich materials need positive charges and electron-poor materials need negative charges. We can control the adsorption/desorption process using the external electron charge device.

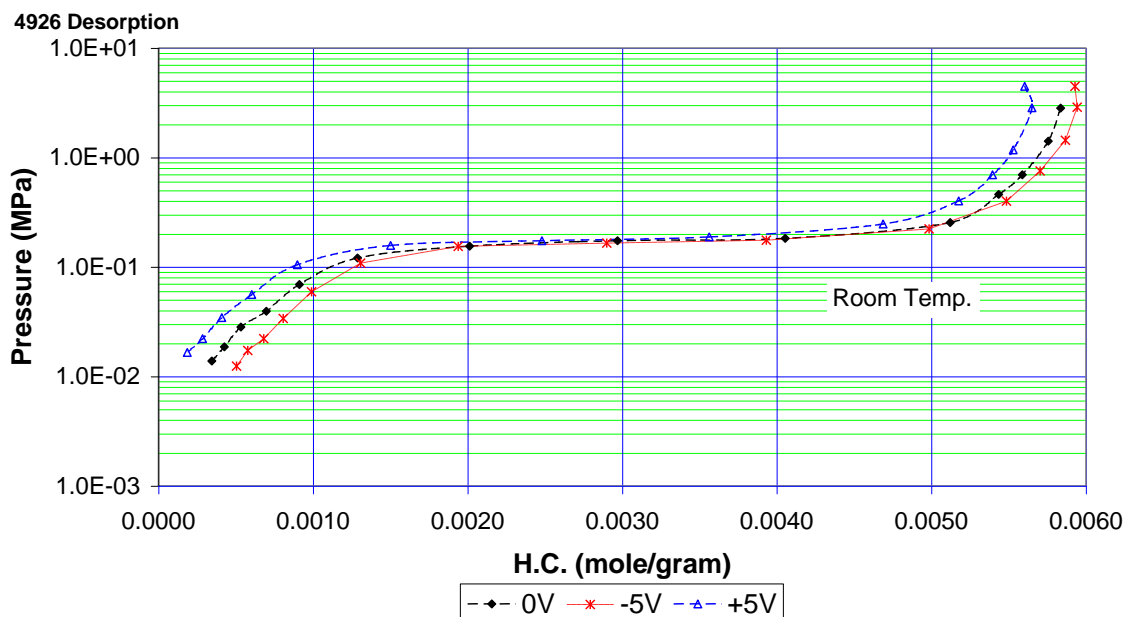


Figure 14. Hydrogen Desorption PCI Curves under Different Voltages

2) Electrochemical Cell Mode

A trial of hydrogen storage from a hydrogen storage material with electrolyte was performed in the Sievert test station as well.

Dissolve 0.5g PMMA in 5 ml propylene carbonate. Then add 0.532g LiClO_4 . This results in 1M PMMA/1M LiClO_4 solution. The solution was coated onto the stainless steel electric pin inside a nitrogen purged glove box.

Next, 2.0g PMMA was dissolved in 20ml propylene carbonate. Then 2.13g LiClO_4 , 0.186g ferrocene and 0.272g ferrocenium tetrafluoroborate was added. The resulting electrolyte solution is 1M PMMA / 1M LiClO_4 / 0.05M ferrocene / 0.05M ferrocenium tetrafluoroborate. Then 1 gram of electrolyte solution was added to the stainless steel sample vessel with 3 grams of activated hydrogen storage carbon powder.

The sample was loaded into the vessel on the Sievert test station. It was leak checked and calibrated based on the sample vessel's dead volume. A PAR260 potentiostat was connected to the electric sample vessel. The pin is connected to the working electrode. The sample vessel body is hooked to the reference/counter electrode. This is a two electrode setup. A dynamic PCI curve was acquired every 30 minutes and the results are displayed shown in Figure 15. At the end of each point, a cyclic voltammogram (CV) was taken with the potentiostat. Figure 16 contains the CV comparison of the hydrogen storage cell under different pressures. A capacitance characterization is observed from the figure. **Therefore, the external charges should affect the storage material substrate.** Initially, the CV curves between 1.8psig and 323psig pretty much overlap with each other, while at higher pressure, the current increases. The reason is probably due to high pressure making the contact of powder with electrodes better. At pressure points above 323psig, the curves began to change from capacitive to resistive. Resistance became smaller at higher pressure. However, after the pressure is greater than 528psig, the current decreases (Figure 17). The effect could be due to increased hydrogen

adsorption, which reduces the storage material's conductivity. The experiment verified that the external charge with electrochemical cell mode did affect the hydrogen storage.

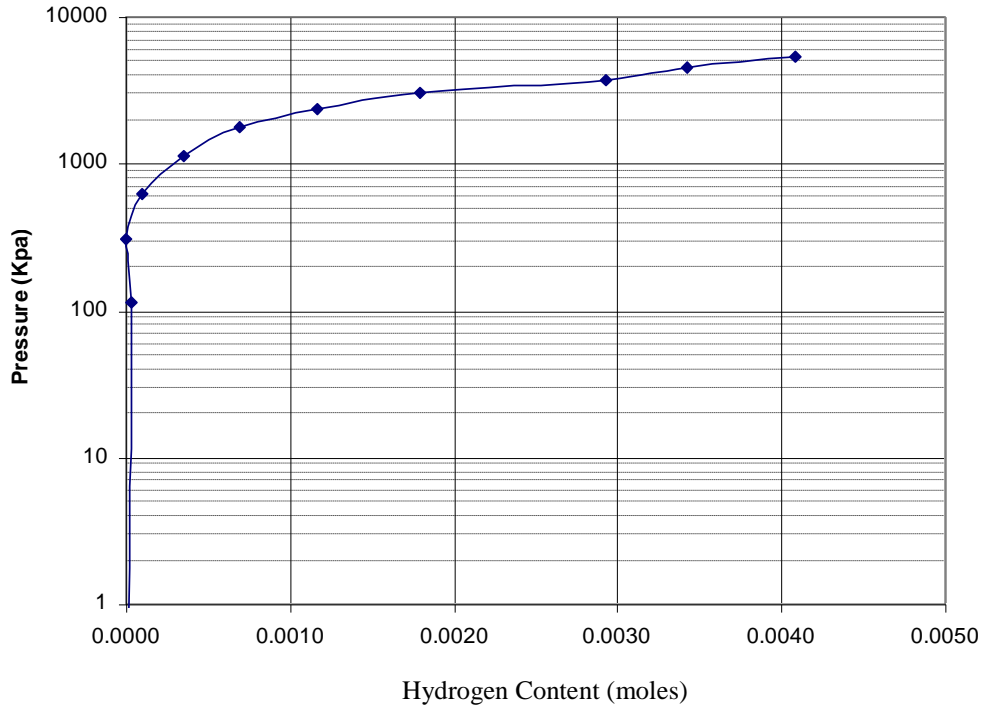


Figure 15. PCI Curve of the Carbon Cage Framework Material for Hydrogen Storage

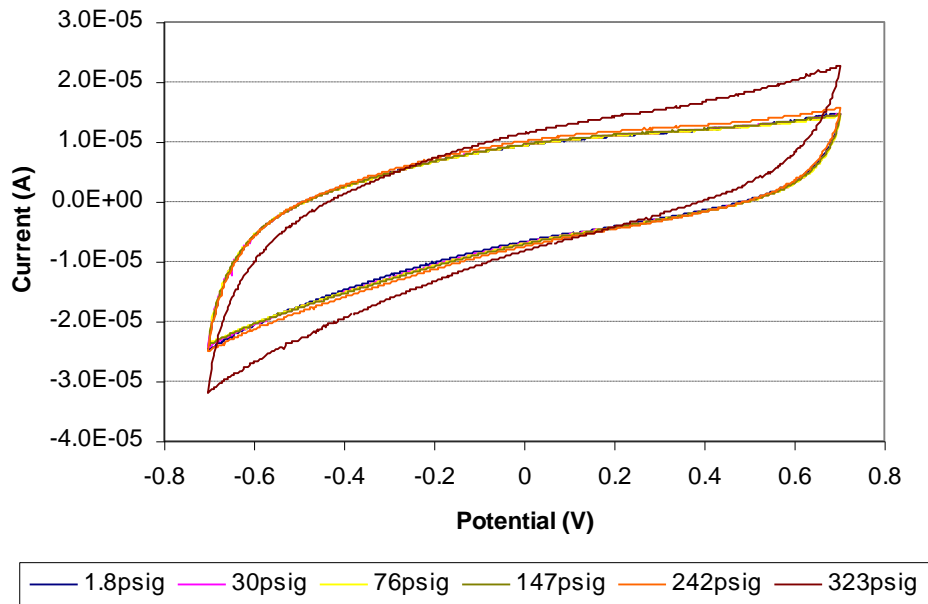


Figure 16. Cyclic Voltammograms of the Hydrogen Storage Cell under Different Pressures

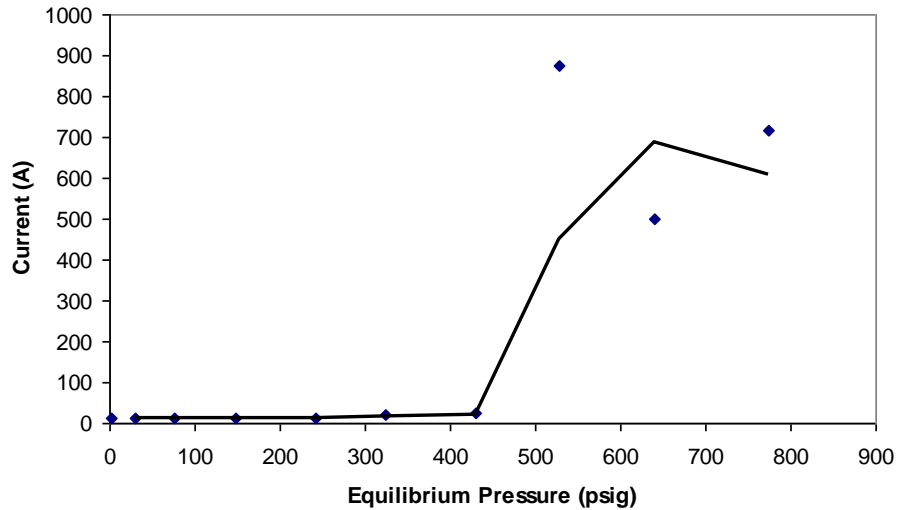


Figure 17. Electron-charge Current under Different Storage Pressures in the Hydrogen Storage Cell

3). Liquid Gel Carbon Material and High Surface Carbon Materials

The liquid gel carbon cage material as described in the above was placed in two Sievert devices for the hydrogen storage tests under different temperatures. The samples were doped with approximately 10% Fe/0.3% Pd and 10% Fe/0.1-% Pd,10% Ti alloy respectively. Figure 18 contains the dynamic pressure-concentration-isotherm curves of the Fe doped liquid gel carbon materials. This dynamic test reduces the test time, i.e. points were taken with 30 minutes interval. The storage capacity of the material increases as the temperature decreases. A 0.6 Wt.% hydrogen storage capacity was obtained at the liquid nitrogen temperature (77K). Ti alloy in the carbon gel material increased the hydrogen storage capacity as shown in Figure 19. The storage capacity is more than 1% at 77K. A metal hydride storage plateau was observed. From the comparison of Figure 18 and 19, lower temperature help the physic-sorption of hydrogen on carbon based material, but the metal alloy composition has less effect at the lower temperatures.

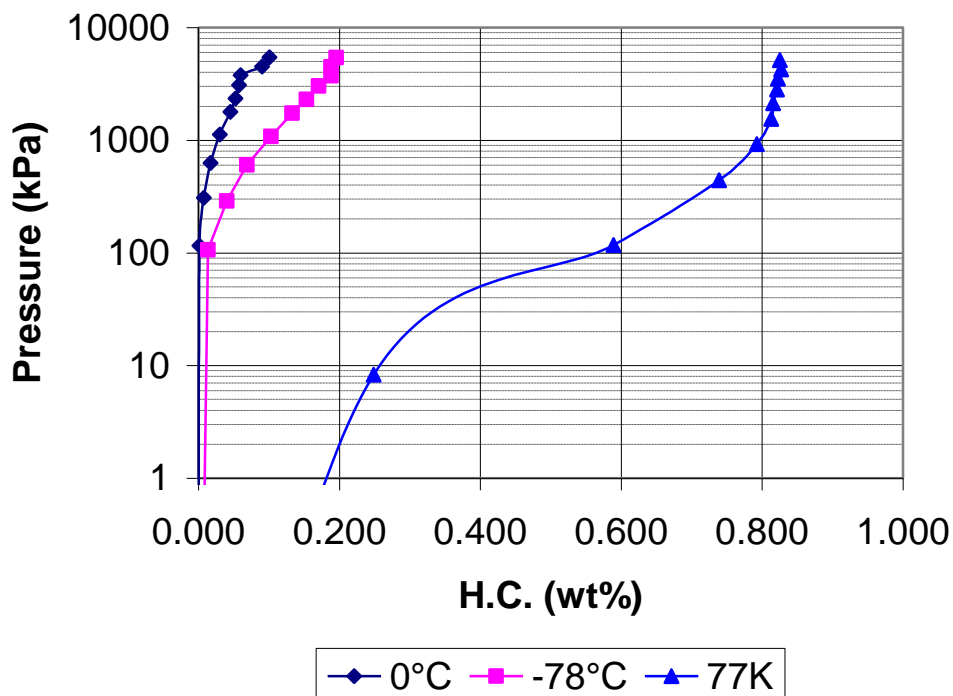


Figure 18. PCI Curves of the Hydrogen Adsorption on Liquid Gel Carbon Cage Framework Doped with 10% Fe and 0.3%Pd, i.e. Sample A

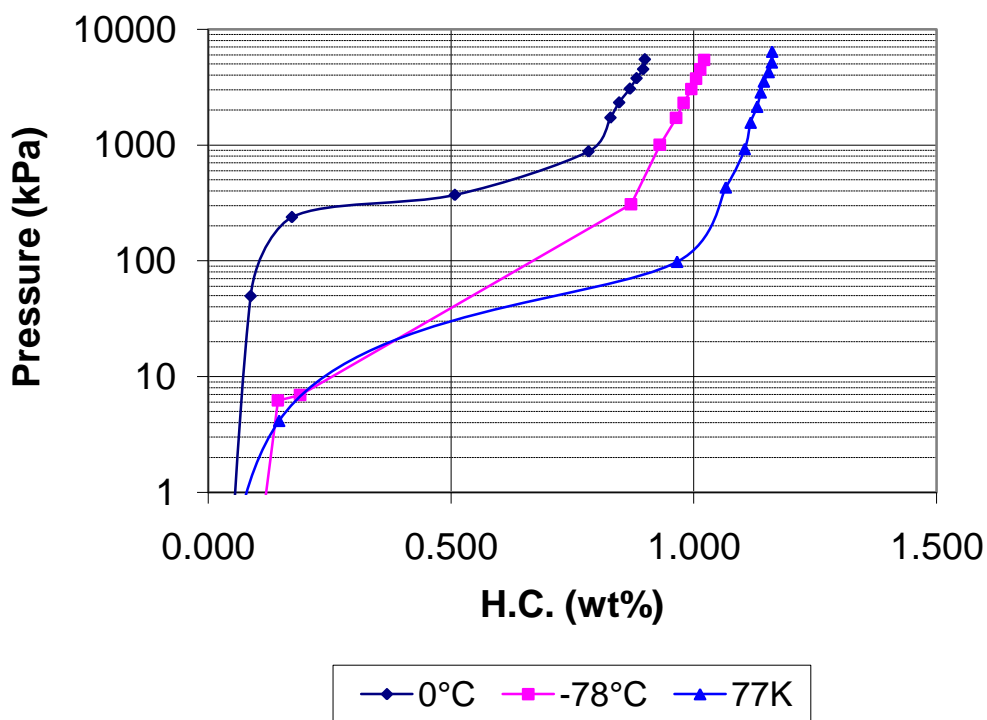


Figure 19. Hydrogen Adsorption on Liquid Gel Carbon Cage Framework Doped with 10% Fe, 0.1% Pd, 10% Ti Alloy, i.e. Sample B

Samples from SUNY Syracuse, APKI-N3 and APKI-N5, were put into the Sievert test station to acquire hydrogen adsorption PCI curves at room temperature, dry ice temperature and liquid nitrogen temperature. The PCI curves at low temperature were corrected for the un-immersed portion of the sample vessel. Testing under different temperatures allows us to determine the hydrogen absorption energy of each material. These two samples performed very similarly. SEM analysis reveals that the SUNY-Syracuse sample has a nano-smooth surface (Figure 21). The element mapping shows only carbon is present in the sample (Figure 22).

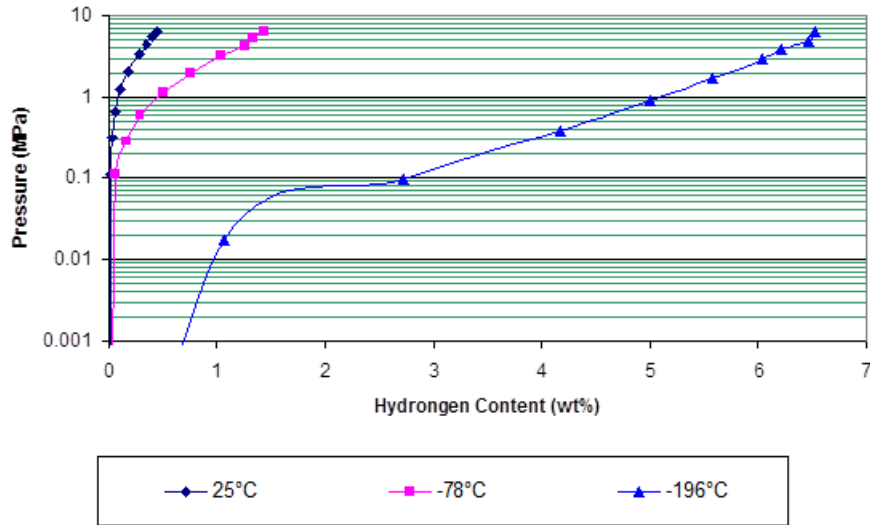


Figure 20. PCI Curves of SUNY-Syracuse Sample APKI-N3 under Different Temperatures

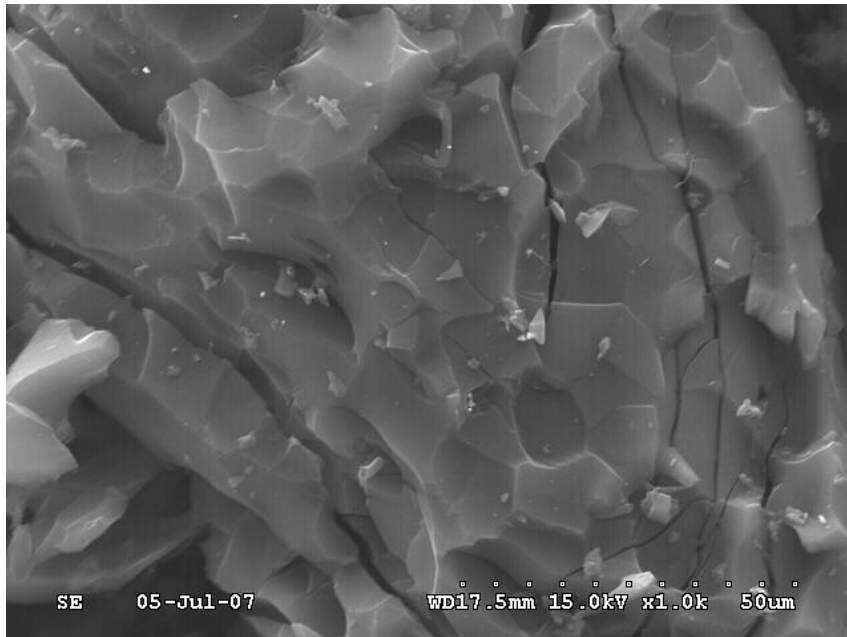


Figure 21. SEM Image of the SUNY-Syracuse Sample

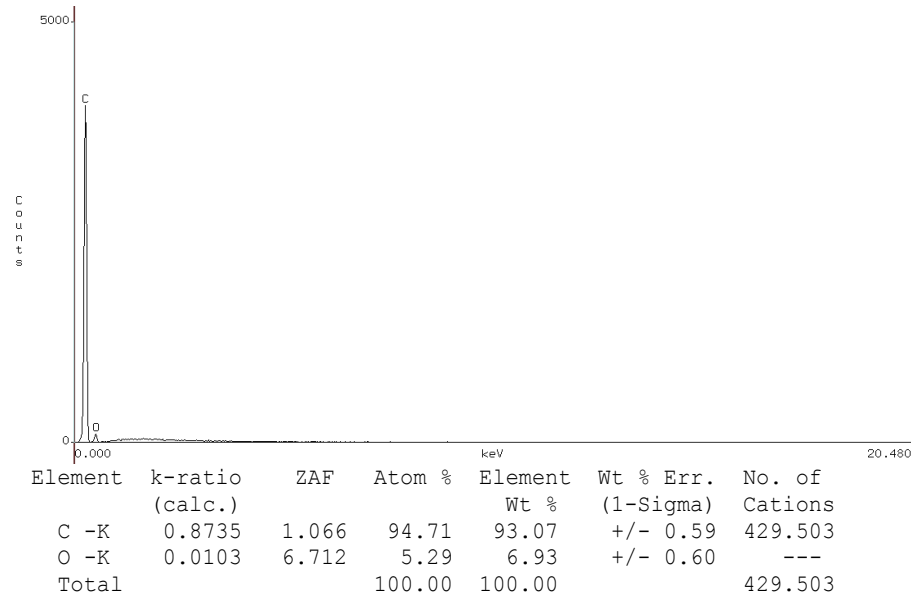


Figure 22. SEM Element Mapping of the SUNY-Syracuse Sample

GTI analyzed the electron-charge distribution on the hydrogen storage samples. In order to improve the electron charge effect on the hydrogen storage, the material particle surface must be charged as shown in Figure 23. Since most of the hydrogen storage materials are electrically conductive, a very thin layer of polymer was coated onto the particles similar to printer toner particles. Table 3 lists the characterization of the charge control agent (CCA). The charge control agent (CCA) was added to the high surface carbon material from Prof. Cabasso's group of the State University of New York at Syracuse and was tested to observe the charge effect on the hydrogen storage based on the physi-sorption. Figure 24 shows the PCI comparison of the hydrogen storage with and without the CCA. When the hydrogen pressure was increased to 3300kPa, the hydrogen storage capacity increased with the addition of the CCA. At 6300kPa of the hydrogen storage rate increased from 0.463 wt.% to 0.609 wt.%, i.e. a **31%** increase.

Therefore, we are working with SUNY to improve the hydrogen storage capacity at room temperature and hopefully we can enhance the storage capacity. The SUNY sample was also tested with CCA in the electron-charge device. At a hydrogen pressure around 6300kPa, the PCI curve with an applied -600V stores more hydrogen (1.8% increase) than the one without applied voltage (Figure 25).

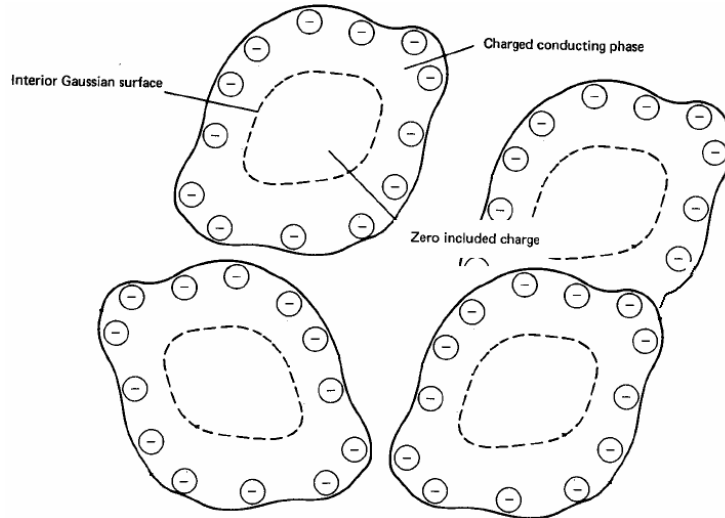


Figure 23. Schematic of Charged Particles for Hydrogen Storage

Table 3. Characterization of Charge Control Agent

Item	Results
Appearance	Black powder
Charge Measurement 60 seconds (- $\mu\text{C}/\text{g}$)	40.0
Average particle size (μm)	1.58
Apparent specific gravity (g/cm^3)	0.295

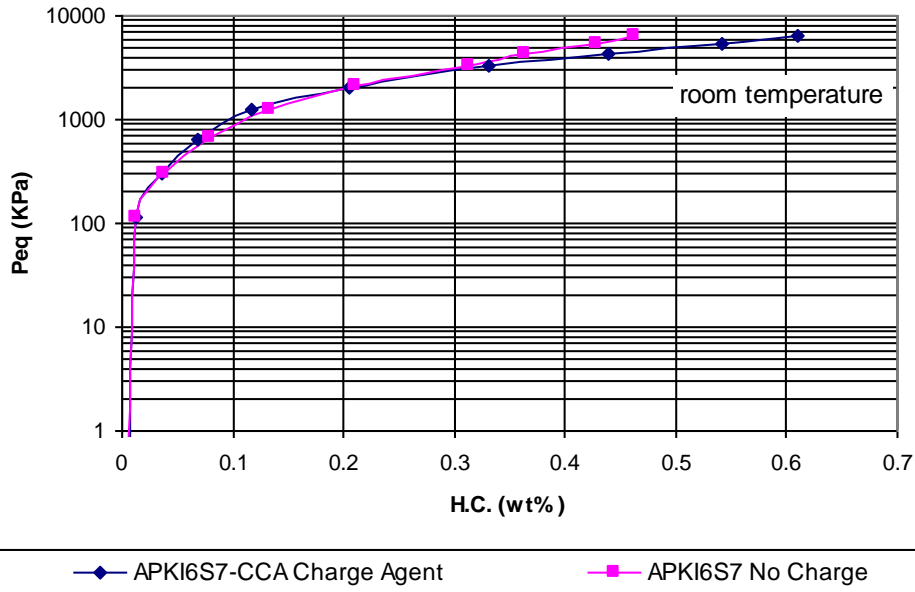


Figure 24. CCA Effect of Hydrogen Storage on the High Surface Carbon Material

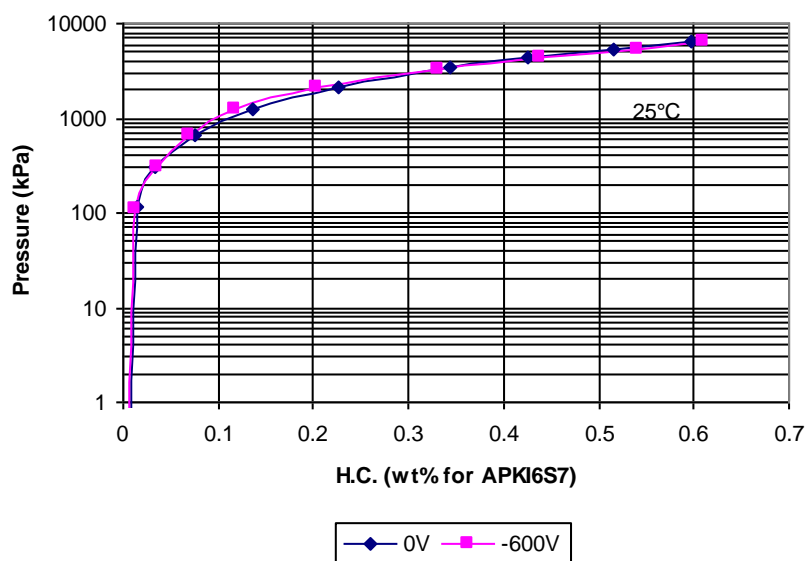


Figure 25. External Charge Effect on the Hydrogen Storage of SUNY Sample

The Metal hydrogen storage materials were also tested using the CCA modification. The hydrogen uptake and release cycles improved the hydrogen storage capacities from 0.45wt.% to 0.62 wt.% (Figure 24) (approximately 37% increase); the CCA binding to the metal based materials changed the metal surface electron distribution. **We can conclude here that the CCA increases the hydrogen storage not only from carbon based but also from the metal based materials.**

A high surface area carbon from our industrial partner AMTI was tested for hydrogen storage capacity. 50 g samples enabled us to do a series of experiments to find the trends of physical and chemical modifications. The carbon has a surface area of 1176m²/cc, with a nitrogen micro-pore volume of about 0.4cc/g and most of the pores are 0.5~0.8 nm. The measured density is 1.13g/cc. A cold steel chisel and hammer was used to chip pieces off of the material. The pieces were then crushed in a stainless steel die with a hydraulic press and sieved with a 40mesh screen sieve. The particles less than 40 mesh were collected and tested in the Sievert Station or processed further for testing. The PCI curve of the sample crushed to less than 40 meshes is displayed in Figure 26. The hydrogen storing capacity of the carbon at room temperature was approximately 0.34 wt%. The sample was also tested at 77K as shown in Figure 27 and 2.7 wt% hydrogen storage capacity was observed. The ATMI samples were modified with the charge control agent (CCA) and an increase in the hydrogen storage capacity was observed as demonstrated Figure 28. It is likely that the CCA had good contact with carbon material after long time milling.

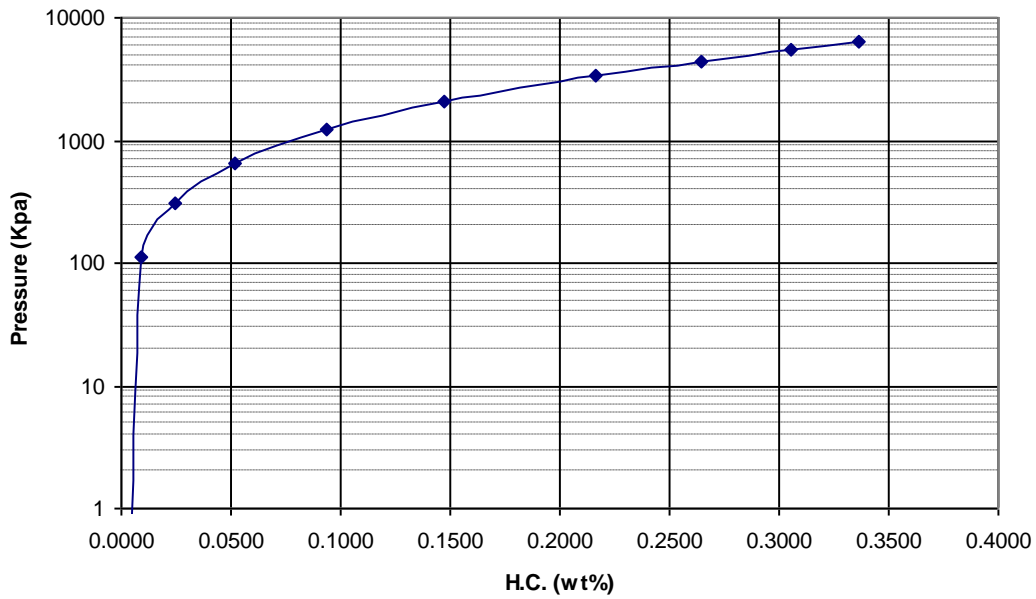


Figure 26. PCI Curve of AMTI Carbon for Hydrogen Storage at Room Temperature

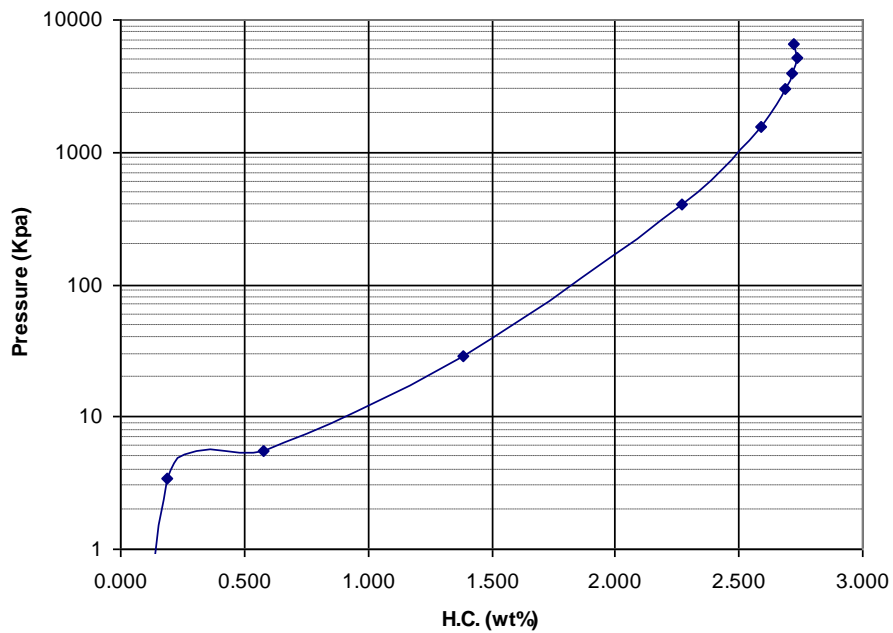


Figure 27. PCI Curve of AMTI Carbon for Hydrogen Storage at 77K

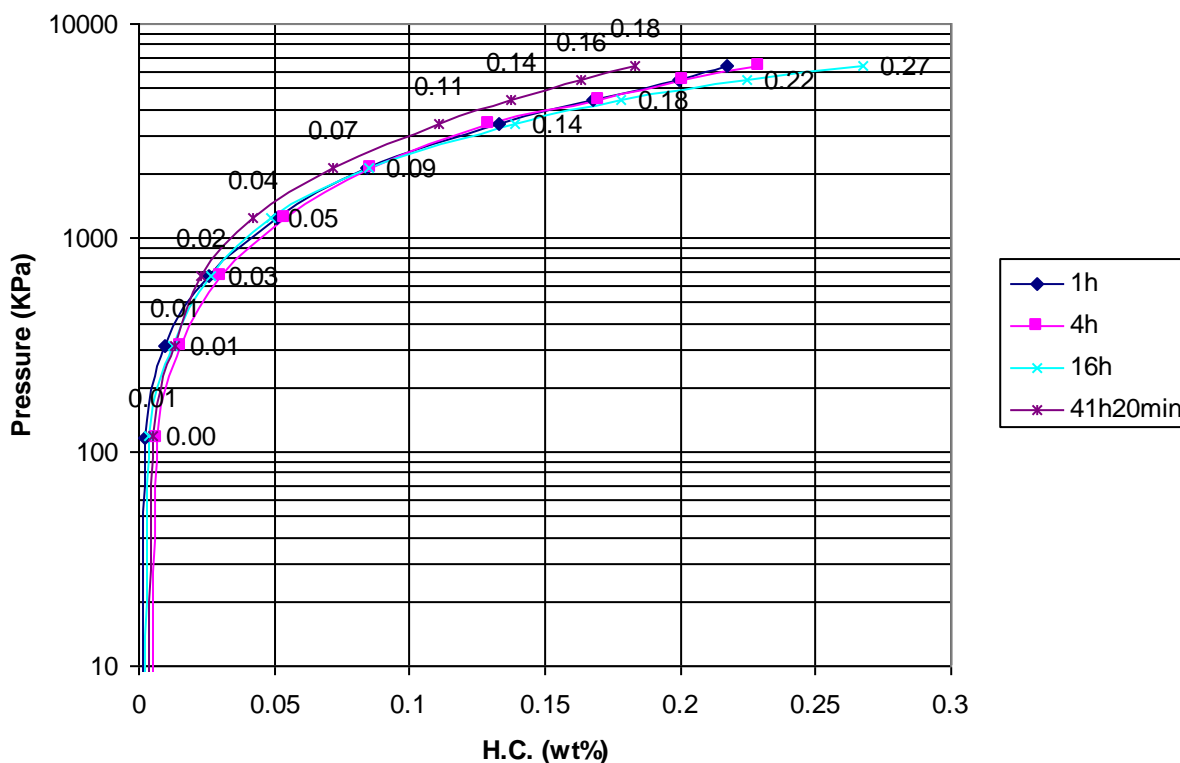


Figure 28. PCI Curves of an ATMI Sample at room temperature under Different Milling Times

The carbon-based materials were modified with electron-rich materials and electron-charges were applied to the substrate. At high voltage, it was found that the metal modified AX-21 with charge control agent (CCA) increased the hydrogen storage capacity; however, the control AX-21 with CCA, (not metal modified), was not sensitive under high voltage as shown in Figure 29. The PCI curves at room temperature for the metal modified AX-21 material without the CCA are displayed in Figure 30. The results from these curves demonstrate that the positive charge increases adsorption on the metal modified AX-21 at room temperatures. At 77K, the hydrogen storage showed the same trends but stored less hydrogen (only about 0.45%). The PCI curve at 77K is displayed in Figure 31.

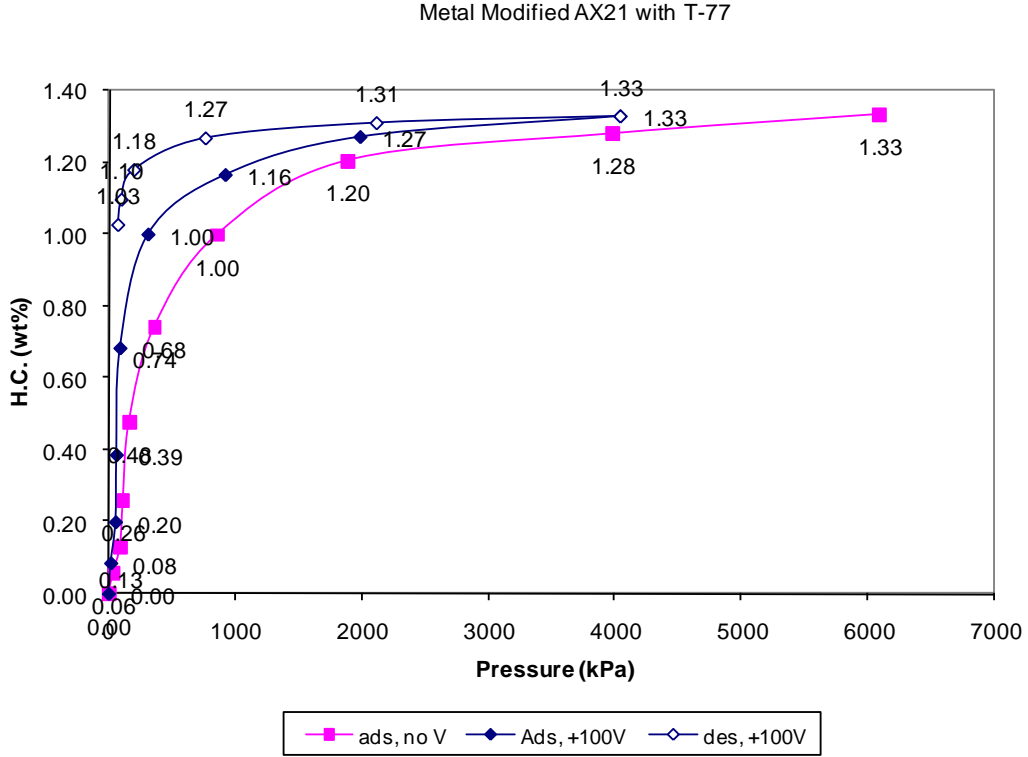


Figure 29. Electro-static Voltage Effect on Hydrogen Storage at Room Temperature

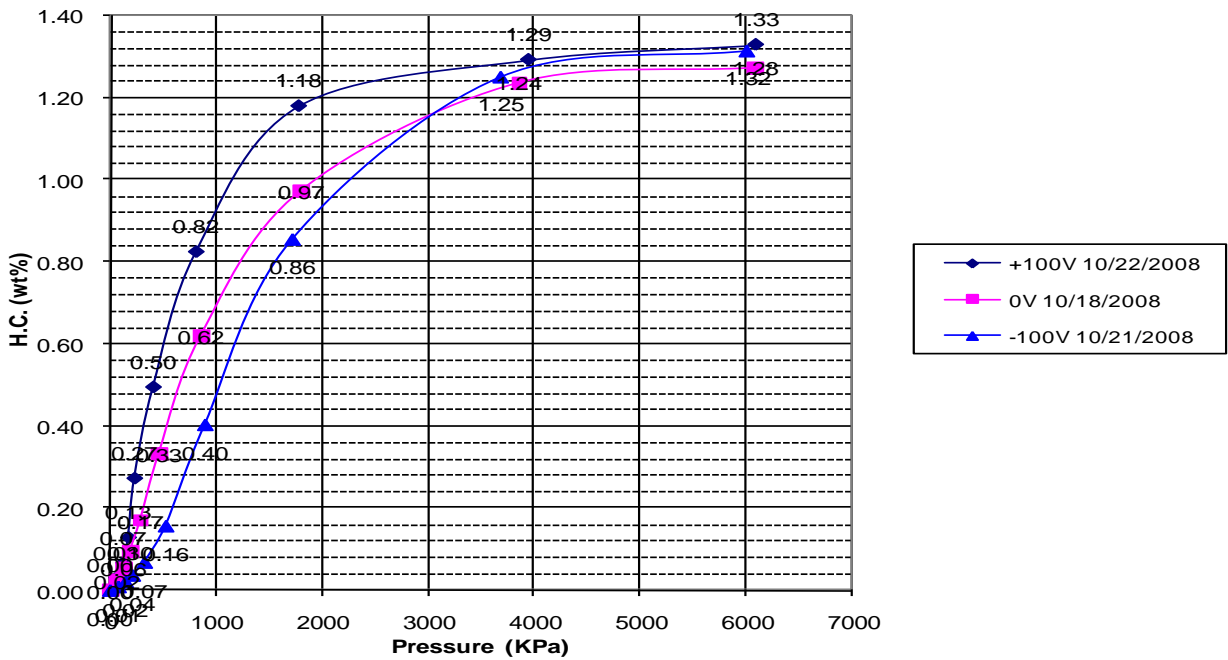


Figure 30. Electro-static Voltage Effect on Hydrogen Storage at Room Temperature for metal modified AX-21 without a CCA.

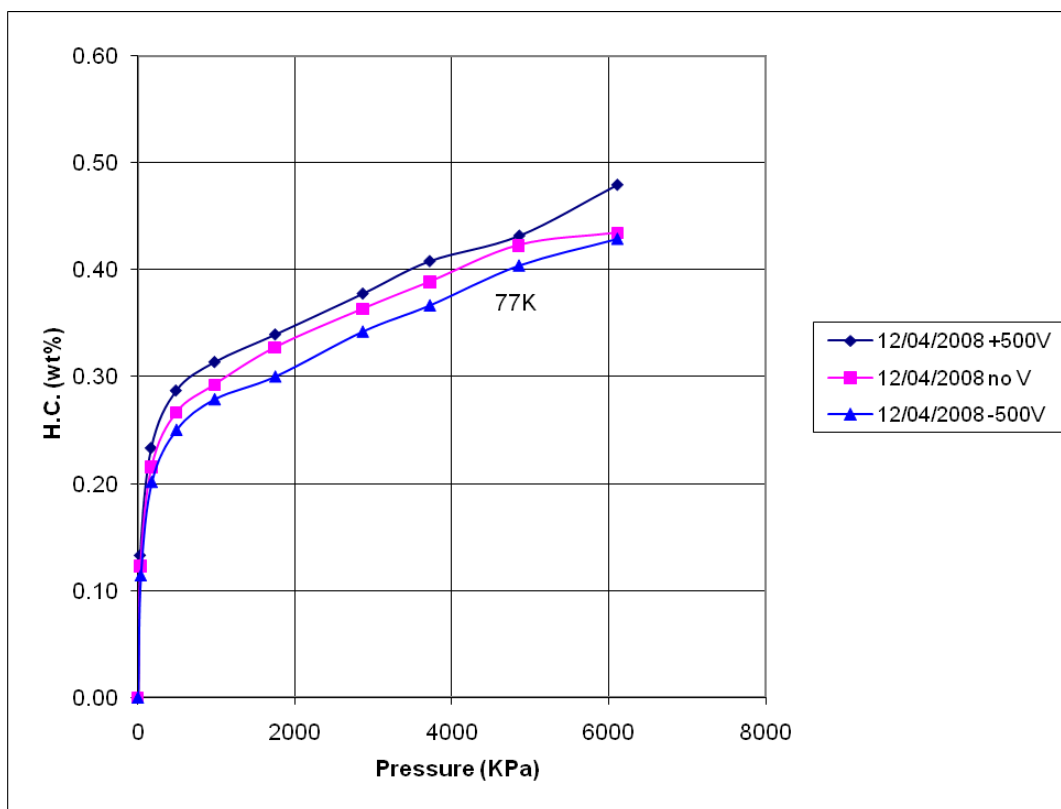


Figure 31. Electro-static Voltage Effect on Hydrogen Storage at 77K

SUNY samples were tested in Sievert test station. All the samples were tested at room temperature and liquid nitrogen (77K) bath. Table 4 summarizes the results from the SUNY sample tests. It was concluded that APKI6S2 had the best hydrogen storage capacity of 6.98 wt% at 77K. APTPN1 also showed 6.42 wt.% hydrogen storage at 77K.

Table 4. Summary of SUNY samples at 6300kPa

Sample name	Room Temperature (wt%)	77K (wt%)
APPANNI(2)	0.52	6.49
APKI6S2	0.40	6.98
MK775	0.44	5.82
PK-NaH-1-1	0.38	4.41
APTPN1	0.49	6.42
N24Ma1045	0.33	4.8
N24	0.52	6.9
APK25N1	0.77	6.0

Borane-Nitride is a very attractive material for hydrogen storage. However, the hydrogenation and dehydrogenation kinetics are slow. The hydrogen release from Borane-Nitride at 80°C is displayed in Figure 32. It took over 24 hours for the material to release 5.7wt% hydrogen. At

900 psi, it took 2.5 hours for borane nitride to decompose and release 1.5wt% hydrogen. When a negative 1kV charge was applied the time was reduced to and only 40 minutes displayed in Figure 33.

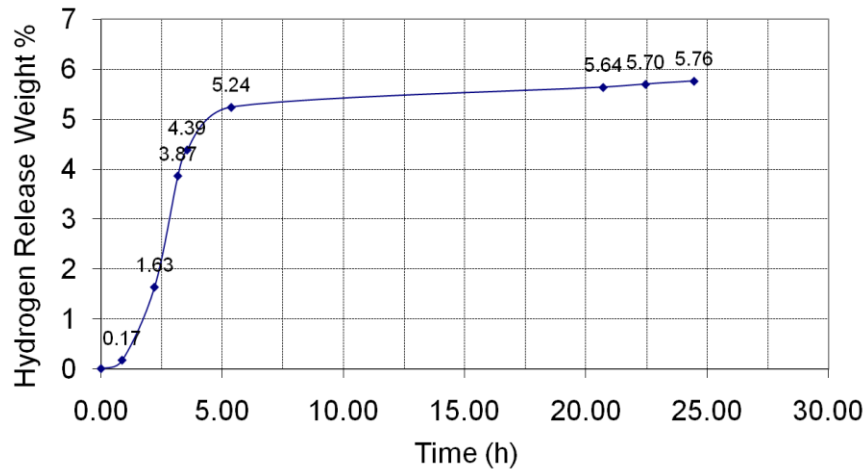


Figure 32. Borane-Nitride Hydrogen Release at 80°C with Time

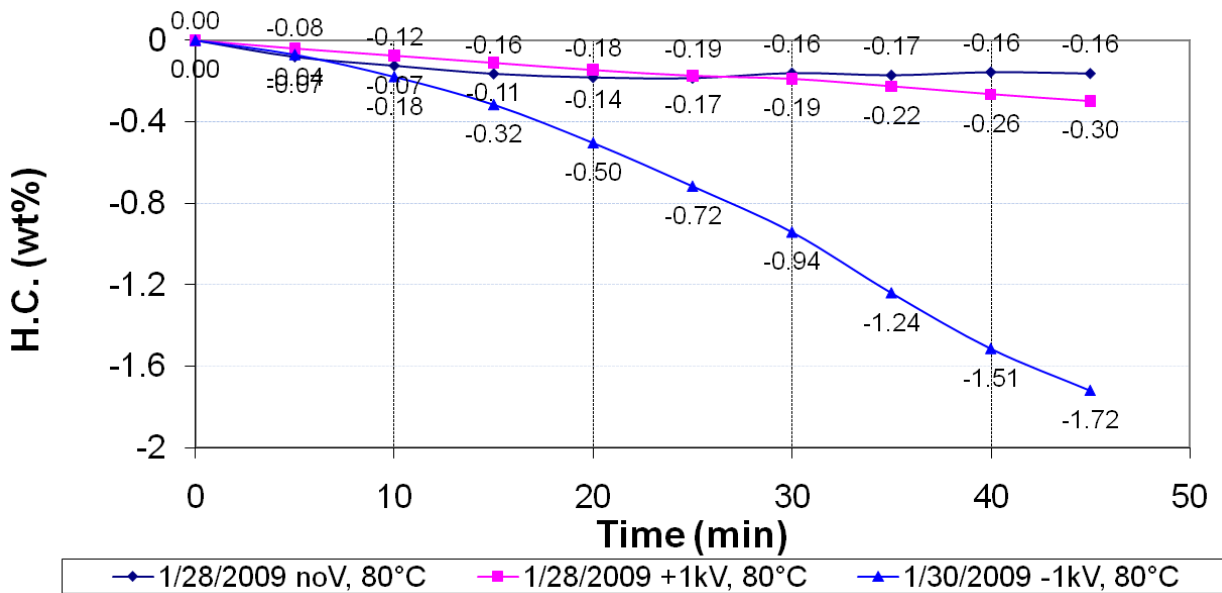


Figure 33. Electro-static Voltage Effect on Hydrogen Release of Borane-Nitride at 80°C and 900psi H₂ Pressure

Figure 34 shows the cyclic voltammograms, which exhibit NO internal short in the system and verify that the adsorption increase/decrease was NON-Faradaic. The CV was taken at 900psi H₂ pressure, 80°C. As scanning continues, the current becomes smaller and smaller, which proves the NON-Faradaic effect on adsorption increase/decrease.

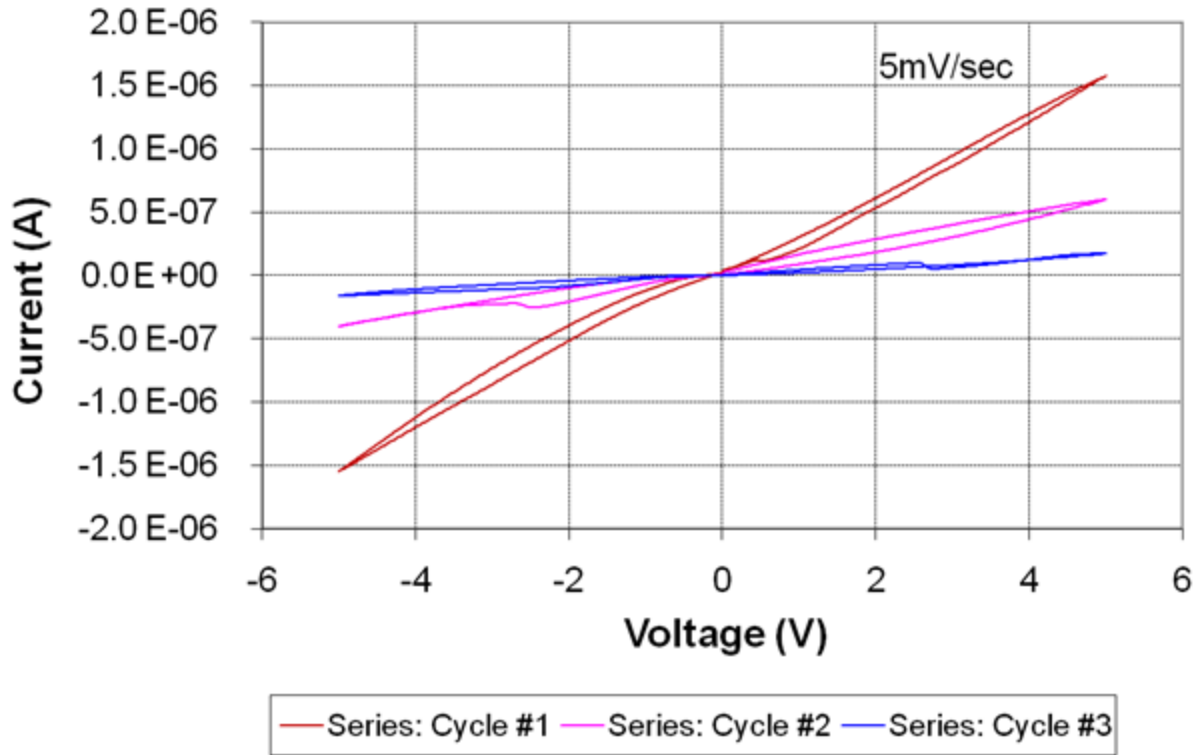


Figure 34. Cyclic Voltammogram of the Hydrogen Storage Reservoir

The electrostatic effect on hydrogen storage with 1.00g borane-nitride and 0.05g catalyst at 80°C is presented in Figure 35. The threshold point occurs when pressure increases to 6000kPa with a negative charge. This figure verifies that the negative charge increases the hydrogen storage of materials.

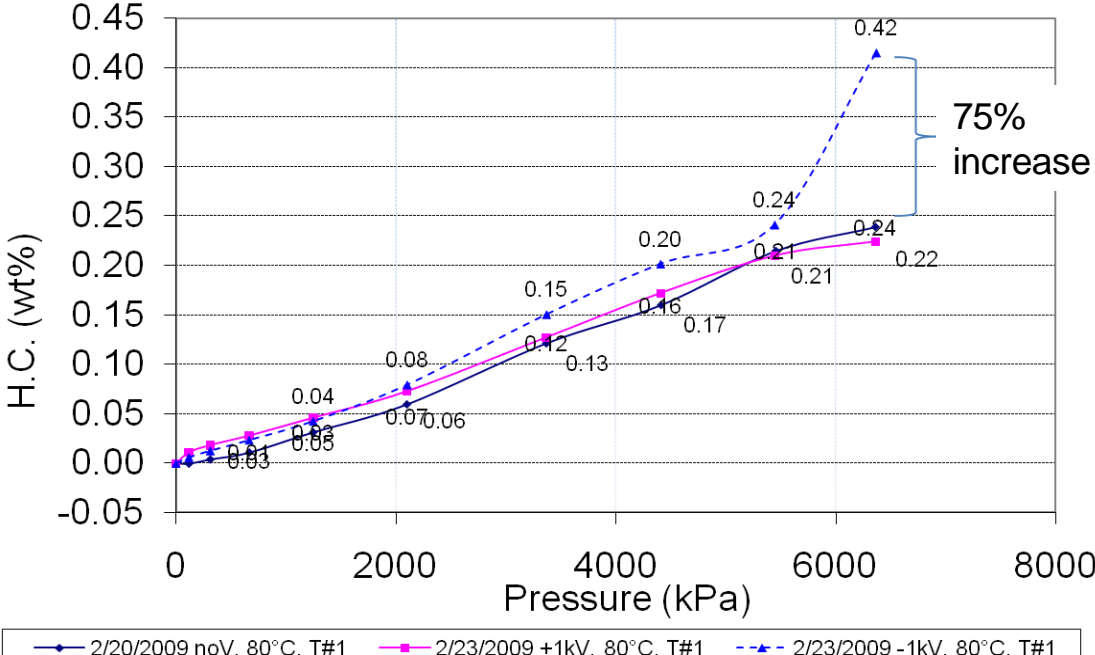


Figure 35. Electro-static Voltage Effect on Hydrogen Storage Material B-N at Room Temperature

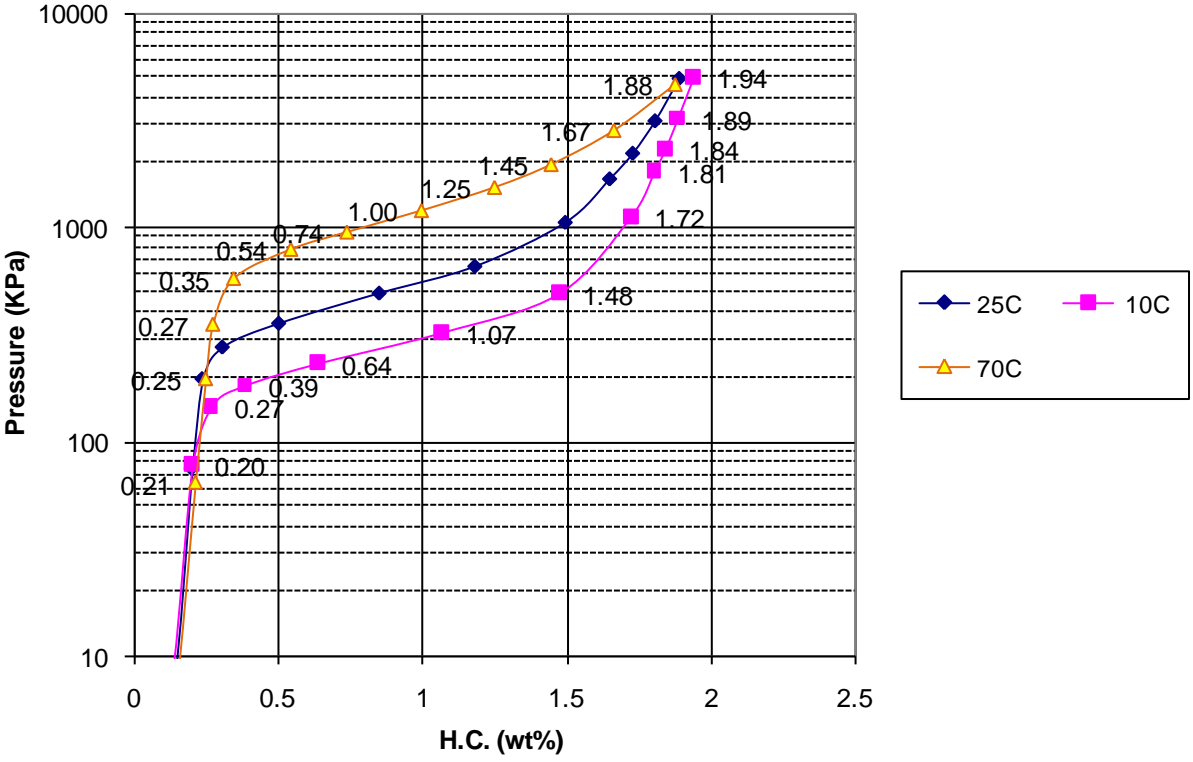


Figure 36. PCI curves of the metal hydride based hydrogen storage material under different temperatures

Figure 36 shows the PCI curves of the hydrogen storage material under different temperatures and demonstrates that the cooling and heating system works well. Figure 37 shows the external charge effect using the system. It is verified again that the negative charge stores more hydrogen; however the positive charge also shifts the PCI curve to left, i.e. more hydrogen stored. The effect could be related to a “non-Faradaic electrochemical modification of catalytic activity”, which somewhat changes the metal material performance. Figure 38 also demonstrates the electron-charge effect on hydrogen storage with the use of a cooling coil. The PCI results show that applied current, especially -0.1A , helps store more hydrogen. Cooling also helps enhance hydrogen storage.

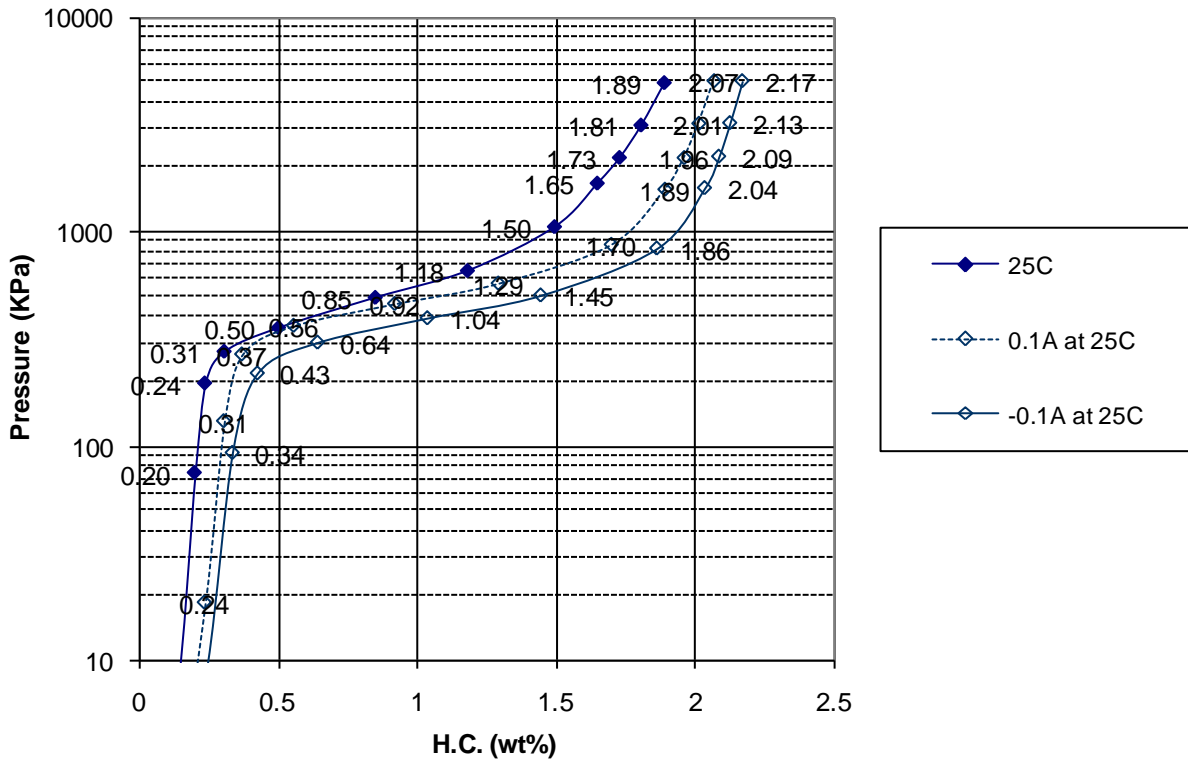


Figure 37. PCI Curves at 25°C under external electric charges

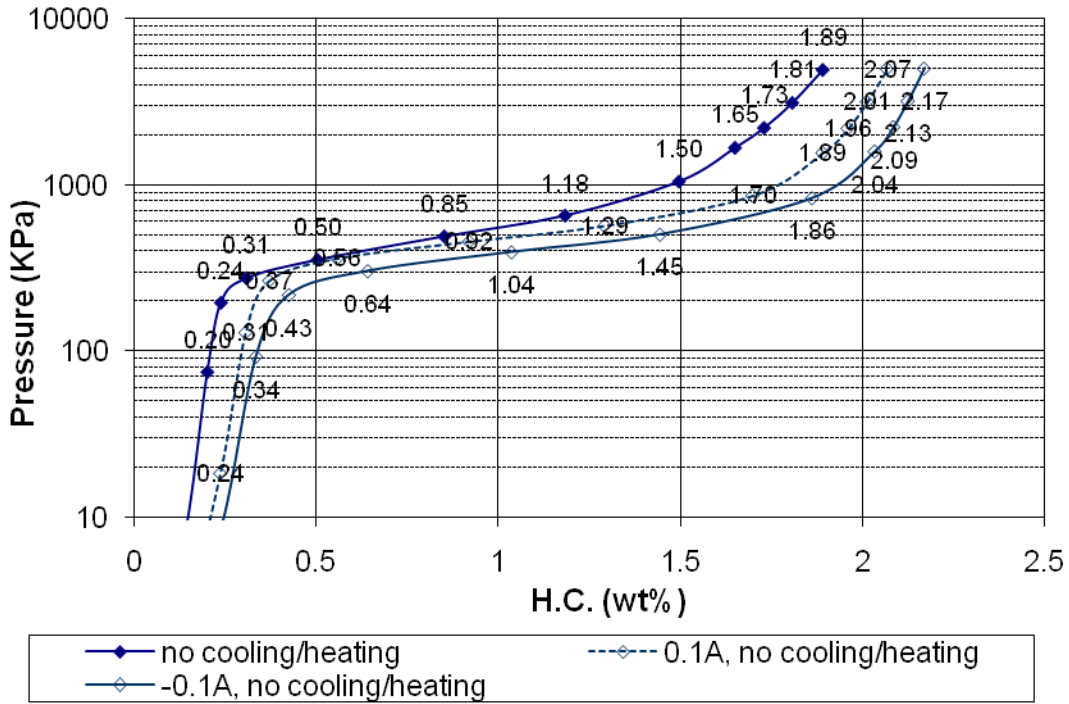


Figure 38. PCI curve of a metal hydride with different current without cooling/heating

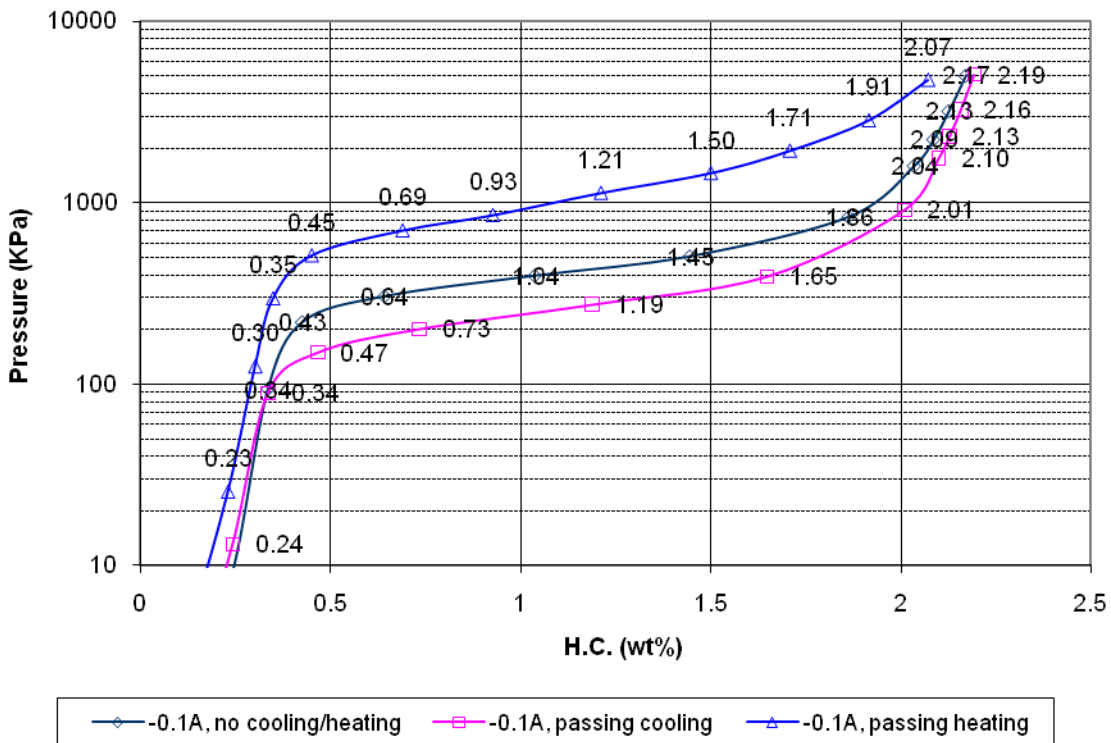


Figure 39. PCI curve of a metal hydride with/without heating/cooling with -0.1A current

A modified sample vessel was kept in an ice water bath to maintain constant 0°C temperature. PCI curves of a carbon-based material were acquired while applying constant voltage of 1.5V, 0.8V and no applied voltage, which is open circuit voltage (OCV). We waited 10 minutes for each data point. The PCI curves showed clearly the effect of applying voltage. With 0.8V applied, the system stores more hydrogen. With 1.5V applied, the system stores less hydrogen. This effect is demonstrated in Figure 40.

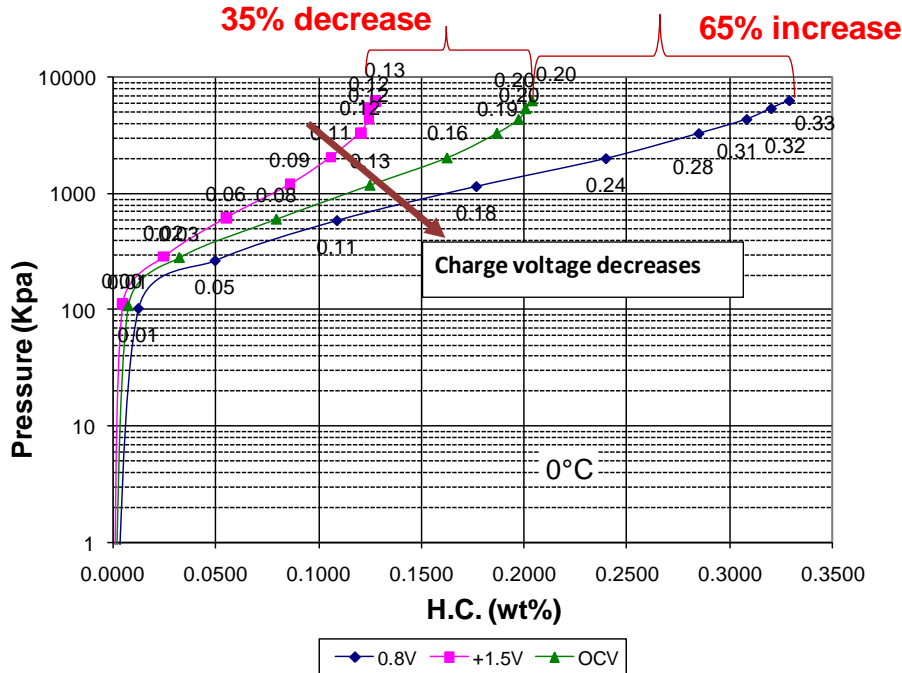


Figure 40. PCI curves of the electrochemical hydrogen storage device under various voltages

After the system was left at steady state with system pressure of 80 psig, a voltage of 0.8V was applied to pin and system pressure was recorded. After some time, a voltage of 1.5V was applied and the system pressure was recorded. The pressure was used to calculate the number of moles of hydrogen gas in the gaseous phase of the system. With a decreasing amount of hydrogen in the gas phase, the system is adsorbing hydrogen; with an increasing amount of hydrogen in the gas phase, the system is desorbing hydrogen. The observed gas phase change as a function of time is shown in figure 41. The phenomenon was repeated twice and between two cycles, the system was left at OCV. We have found that the adsorption/desorption cycle is repeatable. Between the two cycles, the system was kept at OCV. At OCV, a small amount of hydrogen gets adsorbed into the system.

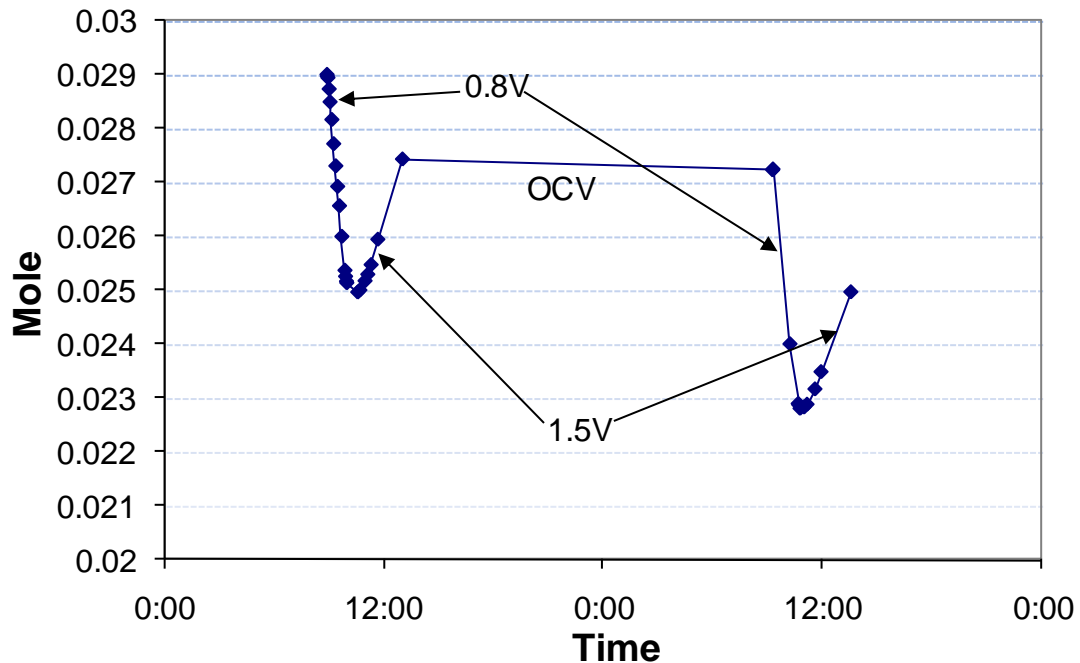


Figure 41. Gas phase hydrogen quantity with time under externally applied voltage

We have also setup a second test system in which we added 0.8g more hydrogen storage material powder at MH side in the sample vessel. We have obtained PCI curves and the steady state chronicle system pressure measurement at adsorption/desorption potentials. The measured chronicle system pressure shows the same trend as measured in the first test system that has only MH. However, we found that it takes a precondition of fully charging the system in order to get a significant amount of hydrogen in and out of the system.

The external charge effect on the hydrogen storage material is shown in Figure 42. A 65% increase in hydrogen capacity was obtained, however the base storage was small (only 0.2 wt.%). The figure shows the steady state test to see the charge change versus the hydrogen pressure in the hydrogen storage reservoir. The charge effect was reversible. We tested the metal hydride with base storage at 1.2 wt% in the system and found that when the voltage decreases the PCI curve shifted and shows more hydrogen storage at the same pressure. These results are shown in Figure 43.

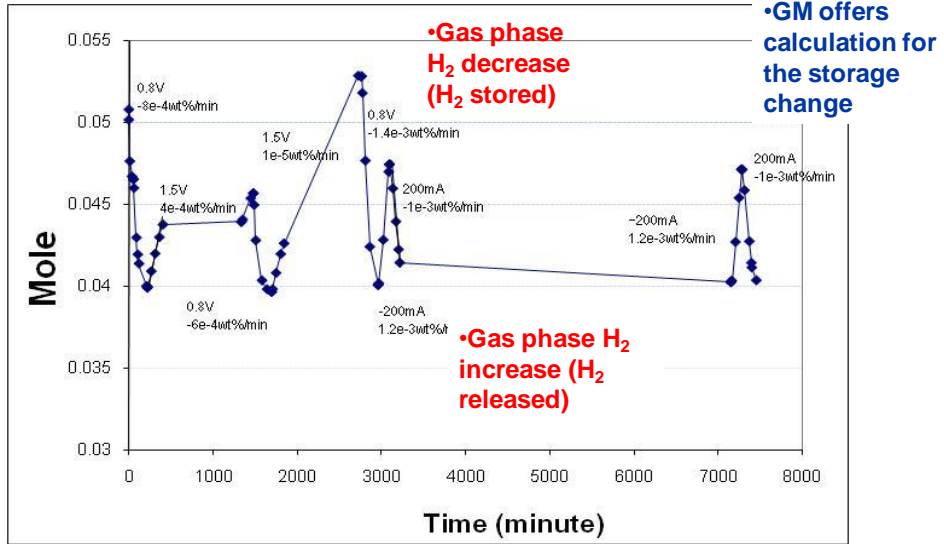


Figure 42. Steady state effect of external charge for hydrogen adsorption and desorption

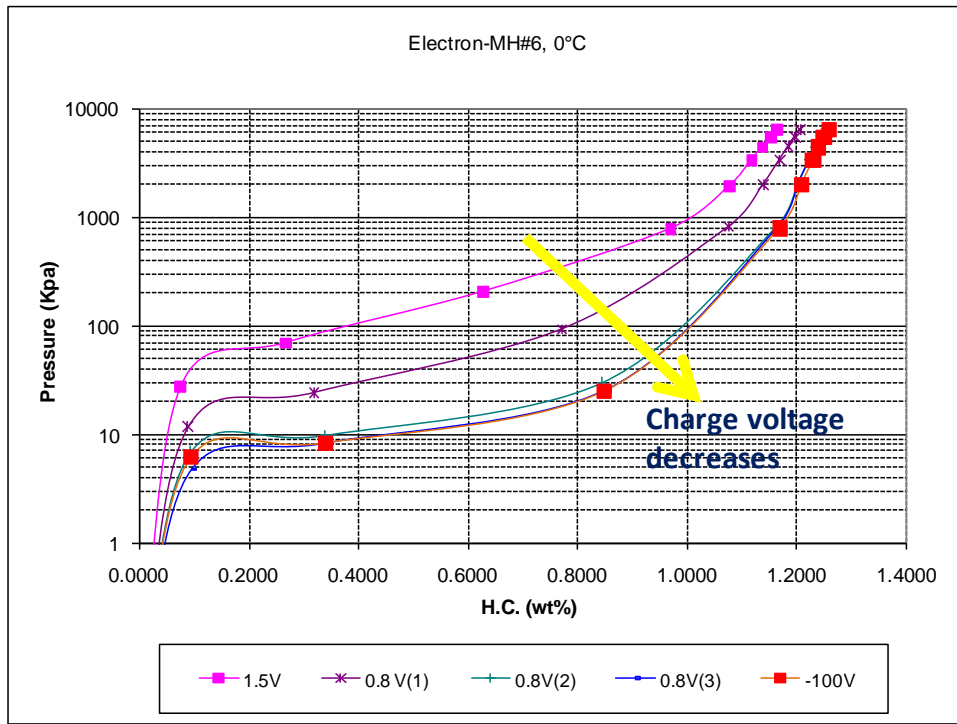


Figure 43. PCI curves of a metal hydride storage material under different external voltages

A new system was assembled to do steady state experiments. We selected three starting points to do steady state tests: 150 psi, 75 psi, and 15 psi, at which the MH was balanced. Figure 44 shows the external charge at 1.5 V (hydrogen desorption) and 0.8V (hydrogen adsorption) under different starting pressures. The accessible hydrogen is 0.87 wt% by using external charge

control. Under the voltage, we can see the system pressure changes, which mean the hydrogen storage capacity changes.

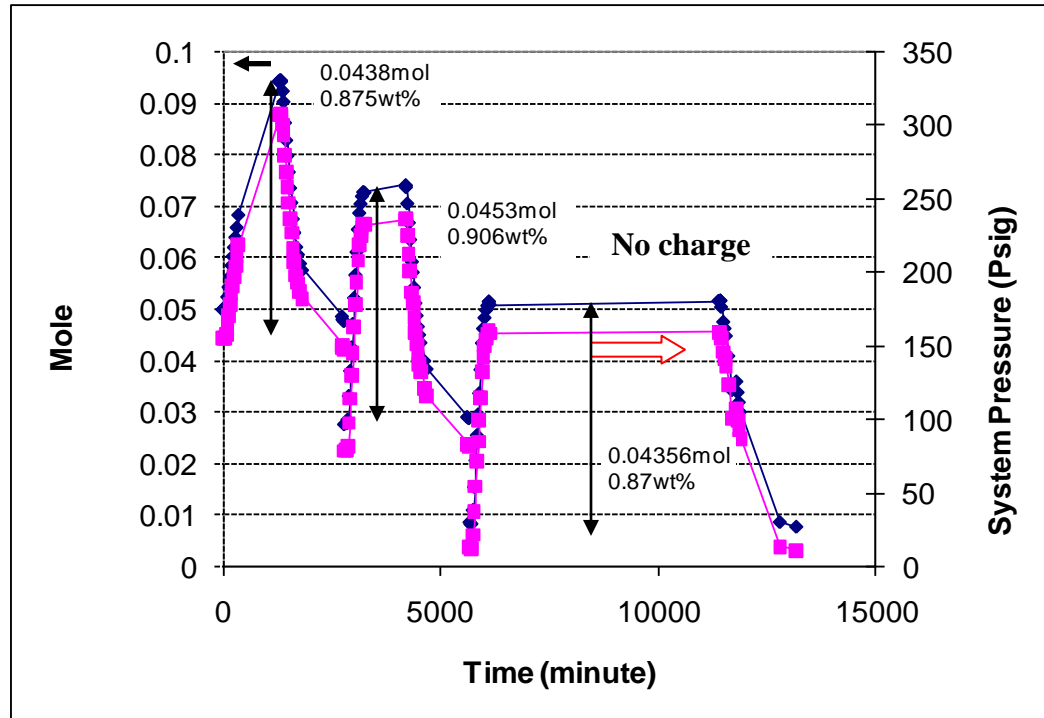


Figure 44. External Charge Effect on Hydrogen Storage at Steady State

The question is whether the hydrogen storage capacity is 1.0 wt% at 15 psi plus 0.87 wt% using external charge (total 1.87 wt%) or NOT. The hydrogen pressure changes under external charge (Figure 44) showed that the hydrogen was the access hydrogen (0.87 wt%), which can be used. The residue of hydrogen storage at 15 psi (1 wt%) could be released by other means, such as heat. Table 5 summarized the results.

Another question is if we increase the MH hydrogen storage capacity or use other hydrogen storage material, does the external charge have the addition of more hydrogen adsorption/desorption? Thus we tried MgH_2 material as shown in Table 6. The external charge changes the hydrogen storage capacity.

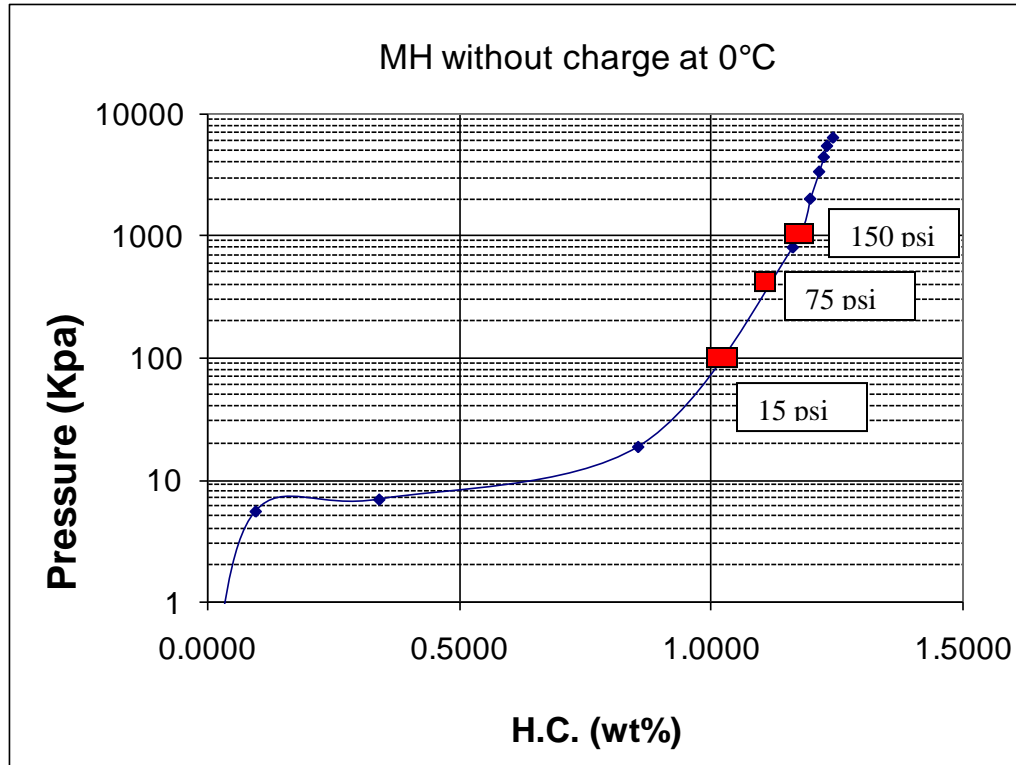


Figure 45. PCI curve of the metal hydride for electron-charge experiment

Table 5. Summary of External Charge Effect on JSW MH6

Start pressure (PSI)	H2 Storage capacity from PCI curve (wt%)	Final Pressure (PSI)	Pressure Difference (PSI)	Storage Capacity Change (Wt%)	Percent of Storage change (%)
15	1.0	165	150	0.870	87
75	1.1	225	150	0.906	82
150	1.2	300	150	0.875	73

It took total 378 min for 150 psi changes. Temperature was controlled at 0°C

The reversibility was very good and reproducible.

Table 6 summarizes the external charge effect on MgH₂. The interesting phenomena observed are the charge effect is reversible; however the kinetics is too slow.

Table 6. Summary of External Charge Effect on MgH₂

Start pressure (PSI)	H ₂ Storage capacity from PCI curve (wt%)	Final Pressure (PSI)	Pressure Difference (PSI)	Storage Capacity Change (wt%)	Percent of Storage change (%)
152.3	7.6 (theoretical)	197.9	45.6	0.28	3.7
<p>At room temperature for 4260 minutes, the pressure increased only 14.6 psi. At 80°C, the pressure changed 31 psi (deduct the temperature effect) and took 1380 minutes.</p>					
<p>It took total 5640 min (four days) for 45.6 psi changes. MgH₂ has very bad kinetics at low T.</p>					

Technical effectiveness and Economic Feasibility

This project has demonstrated the feasibility of using the external charge effect to increase hydrogen storage capacities and kinetics. Experimental results showed the hydrogen storage capacity changes reversibly through the use of external charges. The externally charged mode could be (1) electrostatic charge; (2) ultra-capacitor with low current density; and (3) metal-hydride battery mode with high current density. The energy consumption for hydrogen storage using external charge is (1) < (2) < (3). Since the external charge was used only for hydrogen fueling, the energy consumption could be small. The real world energy consumption for the metal-hydride mode is higher than that of the electrostatic charge and ultra-capacitor mode. This increase of electric energy is to be justified with the increase of the hydrogen storage capacity and the increase of the kinetics of hydrogen storage and release of stored hydrogen.

Actual and Goals

The actual results showed that the use of external charge affects the hydrogen capacity, especially the kinetics of the hydrogen adsorption/desorption on base materials. The external charge can vary the hydrogen storage capacity from several percent to 87% depending on the substrate materials. Since the original hydrogen uptake is so small that even with an 87% increase in uptake, the material is no close to DOE's 2015 target of 5.5wt%. Thus, additional hydrogen storage materials need to be developed. With the development of the base material with high capacity, the external charge could increase the hydrogen storage rate to reach DOE's goal. The project verified the external charge method to change the hydrogen storage capacity is feasible.

The program goal is to develop an external electron charge device that is able to store hydrogen to meet the maximum DOE storage target of 9 wt%. Secondly, after the initial program phases of proof of feasibility, performance optimization, and identified processing steps, costs of production processing will be analyzed for commercial manufacture.

Benefit to Public

Hydrogen as an energy carrier is clean and hydrogen can provide power with minimal air pollution and zero carbon dioxide emissions at the point of use. Current interest in hydrogen stems from environmental and energy policy concerns including global climate change, local air quality, noise and security of energy supply, together with breakthroughs in fuel cell technology. The use of hydrogen greatly reduces pollution, since when hydrogen reacts with oxygen, only energy in the form of electricity and/or heat is produced, no green-house gas or any other particulates would be generated. Water is the only byproduct. Hydrogen can be produced from various sources like methane, gasoline, biomass, coal or water. If hydrogen is produced from water, this becomes a sustainable production system and results in reduction of dependence on foreign oil and increases US energy security. Hydrogen storage plays a key role in the hydrogen economy since once hydrogen is produced, it needs to be stored and transferred to different locations especially if it is used on transporting vehicles. It is crucial to have high storage percent and fast storage/release kinetics to facilitate a hydrogen economy. External electric charge is hereby proved to facilitate hydrogen storage and kinetics in this way.

Summary and Recommendations

The development of hydrogen storage materials is progressing in the U.S. and throughout the world. A fast-fill hydrogen storage method will depend heavily on the type of base materials to adsorb the hydrogen. The external bias to change hydrogen storage capability could be a way to change hydrogen-fill kinetics. The electron-charge method has demonstrated the effectiveness to store and release hydrogen in a fast manner.

The concept of using external charge could be a viable option for improving hydrogen storage capability and kinetics for adsorption/desorption. GTI would recommend DOE to consider more about external bias for hydrogen since new materials for hydrogen storage will take time to be developed. GTI would also recommend DOE consider the potential combination of the external bias with hydrogen filling in a fueling station.